Quantification of spatial and temporal variations in trace element fluxes originating from urban areas at the catchment scale

Claire Froger, Cecile Quantin, Louise Bordier, Gaël Monvoisin, Olivier Evrard, Sophie Ayrault

Quantification of spatial and temporal variations in trace element fluxes originating from urban areas at the catchment scale

Claire Froger[*,1,2,3], Cécile Quantin[3], Louise Bordier[2], Gaël Monvoisin[3], Olivier Evrard[2], Sophie Ayrault[2]

*Corresponding author: claire.froger@inrae.fr

Tel: ± 332 38 41 80 49

Address: INRA, 2163 avenue de la Pomme de Pin, 45075 ORLEANS CEDEX 2

[1] INRAE, US1106 Unité Infosol, Centre de Recherches d'Orléans, CS 40001, Ardon, 45075 Orléans Cedex 2, France

[2] Laboratoire des Sciences du Climat et de l'Environnement (LSCE/IPSL), CEA-CNRS-UVSQ, Université Paris-Saclay, 91191 Gif-sur-Yvette, France

[3] Géosciences Paris Sud (GEOPS), Université Paris-Saclay – CNRS, 91400 Orsay, France

Abstract

Background, aim and scope

The release of trace elements (TE) associated with the development of human activities has accelerated since the 19th century, leading to the pollution of river systems. Despite a drastic reduction in industrial inputs in Northern Europe, diffuse pollution originating from urban areas still prevents achieving the good status required by the European Water Framework Directive. The objectives of the current study, which is a part of a wider project, were to determine the impact of hydrological dynamics on the total exports of TE from an urban catchment and to develop an assessment tool to evaluate the level of contamination of a catchment based on its specific particulate TE fluxes.

Materials and methods

Accordingly, this research investigated the behavior of TE contamination in a 950-km^2 catchment (Orge River, France) showing a strong urbanization gradient in downstream direction. Particulate and dissolved samples were collected in the river during a hydrological year at four stations reflecting the increasing urbanization gradient. Trace element concentrations were measured in the samples using inductively coupled plasma/mass spectrometry (ICP-MS). Daily and annual TE fluxes were calculated at the four stations to evaluate the contribution of urban areas to the total TE exports from the catchment.

Results

The quantification of TE fluxes showed that up to 70% of particulate Cu, Zn, Sb and Pb exported by the Orge River originated from the urban areas located in the lower catchment portions, especially during average water flow periods characterized by frequent rain events. Moreover, the results show that 50% of the dissolved fluxes of Cu, Zn and Pb are supplied by urban areas during the entire year, regardless of hydrological conditions, and that the specific contribution of floods to these fluxes (i.e., the June 2016 event) is lower than that in other catchments because of the continuous supply of dissolved metal fluxes to the river in this urbanized environment.

Conclusion

These results underline the need to integrate all hydrological conditions for the management of TE contamination in urban areas and not to focus on storm events only. Finally, based on a literature survey, the ratios of specific fluxes were homogeneous across different highly urbanized catchments, and they could be used as a tool to compare the levels of anthropogenic pressure in theses contrasted study sites. This observation demonstrates the

similar impacts of societal development on urban river geochemistry worldwide, although they occurred during different time periods.

Keywords: River, metal fluxes, urban runoff, annual fluxes, hydrological regime

1. Introduction

Industrial development has led to deleterious impacts on the environment due to the release of trace elements (TE) into rivers since the 19th century (Nriagu 1996). National and European environmental policies were implemented to protect rivers and reduce untreated wastewater release into watercourses, resulting in a drastic decrease of TE concentrations in the rivers (Le Cloarec et al. 2011; Zachmann et al. 2013). However, diffuse pollution still threatens the good chemical status of rivers in developed countries, especially in urban environments, due to the occurrence of multiple sources of TE (Pistocchi et al. 2019). Specifically, road traffic emissions such as (un)burnt fuels, tires, brake pad wear (Adachi and Tainosho 2004; Adamiec et al. 2016), urban surface degradation (i.e., roofs, roads; Charters et al. 2016) and industrial deposits (Brown and Peake 2006) are considered the main sources of TE delivered to rivers via urban runoff. The Seine River basin in France offers an emblematic example of an early-industrialized catchment that is strongly impacted by human activities because it has been accumulating anthropogenic contaminants for more than a century (Meybeck et al. 2007; Ayrault et al. 2012).

In this context, several studies have attempted to identify the main sources of contaminants in urban watersheds (Van Metre et al. 2008), and others evaluated the contribution of urban pollutants to river contamination (Van Metre and Mahler 2003; Becouze-Lareure et al. 2016). Nevertheless, most of these studies focused on source-specific pathways of TE transfer to the river, such as urban storm water, direct road runoff or roof runoff (Lamprea and Ruban 2011; Charters et al. 2016). At the catchment scale, the evaluation of each pathway's contribution is not straightforward. Therefore, representation of the complexity of urban inputs might be difficult to assess. Moreover, additional contaminant sources such as unmonitored and untreated water releases originating from domestic or industrial sources should be considered (Revitt and Ellis 2016). Therefore, it is important to discriminate among TE sources and to quantify the impact of human activities on river water quality at the catchment scale through calculation of the contaminant fluxes at the catchment scale (Horowitz et al. 2001; Ollivier et al. 2011). Thus far, most pollutant balances have been calculated on an annual basis (Ollivier et al. 2011), and studies were conducted either in notably large catchments with mixed land uses (Horowitz et al. 2001) or in small

drainage areas with a single dominant land-use type (McKee and Gilbreath 2015; Sabin et al. 2005). In the current context of urban sprawl and increasing surface sealing, the need exists to quantify contaminant sources and budgets in urban catchments. Urban streams are more reactive to storm events than rural basins, and the contaminant concentrations in these urban rivers might be strongly variable during single events (Hasenmueller et al. 2017). To improve the management of river contamination, it is necessary to understand the variations of urban inputs during high water stages and extreme events (i.e. floods) characterized by high exports of suspended particulate matter (SPM) (Navratil et al. 2012; Némery et al. 2013).

In this context, the Orge River, a subcatchment of the Seine River basin, was selected because of its high urban pressure (i.e., 5000 inhabitants per km^2 at the outlet) similar to that found in the vicinity of Paris City (i.e., 7000 inhabitants per km^2). The results already published focused on sources of particulate TE using geochemistry tools (i.e. enrichment factors, lead stable isotopes composition) and demonstrated an increasing contamination of suspended particles with TE originating from urban surfaces (Le Pape et al. 2012; Froger et al. 2018). Moreover, the dynamic and sources of polycyclic aromatic hydrocarbons contamination were also studied in this catchment (Froger et al. 2019b, a).

In order to fully understand the behavior of TE contamination in the catchment, the current research addressed the following issues of 1) identifying the dynamics of dissolved and particulate trace element fluxes in response to hydrological changes including the occurrence of an extreme flood, 2) evaluate the level of contamination of the entire catchment using a new assessment tool based on annual specific particulate fluxes.

2. Material and methods

2.1. Study site

The samples were collected in the Orge River catchment presented in Fig1, which drains into the Seine River 30 km southeast of Paris City. Four river sampling sites have been monitored, with three located on the Orge River and one on its main tributary, the Yvette River. The proportion of urban areas rises from 1% to 56% between the upper catchment areas and the outlet. Meanwhile, population densities increase from 300 inhabitants per km^2 at the most rural site (Dourdan) to 5000 inh km^{-2} near the outlet (Viry). Although wastewater is treated mainly outside of the catchment, misconnections in the sewage network are widespread, especially at the outlet, with connection failures estimated at 20% (SAGE Orge-Yvette 2011). The geology of the catchment is characterized by Eocene

formations including carbonate rocks, marls and gypsum, and Oligocene formations dominated by Fontainebleau sands (Schneider 2005; Le Pape et al. 2012).

2.2. Hydrological conditions

Seven sampling campaigns were organized from June 2015 to November 2016 and were selected to reflect the contrasting hydrological conditions observed in the river (Fig S1). Water discharge measured at the outlet varied from 1.6 to 39.7 $m^3 s^{-1}$ with a median value of 3.4 $m^3 s^{-1}$. A water flow class was attributed to each campaign. June 2015 and August 2016 were considered low flow periods (discharge <2 $m^3 s^{-1}$ at the outlet), January and November 2016 were campaigns that occurred during average flow periods (3-5 $m^3 s^{-1}$), and September 2015 and April 2016 were associated with high flow periods (discharge >5 $m^3 s^{-1}$). The sampling campaign organized on 06/06/2016, during the decreasing stage of the June 2016 flood (discharge of 15 $m^3 s^{-1}$ recorded at the outlet), was considered representative of the conditions that prevailed during this exceptional flood.

2.3. River sampling and geochemical analysis

2.3.1. Sampling protocol

First, sediment traps composed of PET bottles submerged in the river, approximately 30 cm under the surface (see Fig S2), for 4 to 5 days were used to collect SPM by sedimentation (n = 27). The suspended solids collected with the traps were decanted, separated from the supernatant and freeze-dried (Gateuille et al. 2014). Suspended particulate matter sampled with sediment traps were shown to be representative of SPM transported in the river (Priadi et al. 2011; Gateuille et al. 2014).

In addition, instantaneous samples of river water were collected during sediment trap installation and recovery (n = 32, 4 per site and per campaign) using 1-L PET bottles and 10-L containers. Concentrations of suspended solids were determined based on the instantaneous samples via filtration at 0.45 µm. In Egly ("E"), water samples were collected from a pipe that continually discharged water into the river ($E_{discharge}$). All flasks and bottles were washed with HNO_3 5% and rinsed three times with ultrapure water before sampling. The bottles were washed several times in the field prior to the sampling. Finally, physico-chemical parameters (pH, conductivity and temperature) were measured during each sampling day.

2.3.2. Sample preparation and geochemical analysis

After filtration (<0.45 µm porosity), aliquots of river water samples were acidified (HNO_3 0.5 N) for TE and cation analysis. The remaining samples were stored for anion, silica and alkalinity measurements. Suspended particulate matter collected with sediment traps were recovered using centrifugation (2800 g) and then freeze-dried.

The total digestion of 100 mg of finely crushed SPM was done in Teflon beakers, with a three-step procedure using first a mixture of HF (4 mL, 30%) and $HClO_4$ (2 mL, 67%) heated at 150°C for 6 hours. During the second step, a mixture of HCl (3.75 mL, 30%) and HNO_3 (1.25 mL, 67%) was added to the samples and heated at 120°C for 3h20. Finally, the third digestion step consisted of three successive evaporations at 110°C of HNO_3 (1 mL, 67%) added to the samples. The solution obtained after digestion was transferred to Falcon® (polyethylene) tubes using 0.5 N HNO_3 to obtain the 50 mL-final volume. To control the mineralization quality, a blank control was included in each digestion batch (22 samples), as well as the Lake Sediment SL1 geostandard (AIEA).

Major elements (Ca, Na, Mg, K, Al, and Fe) were measured using atomic absorption spectrometry in the mineralized SPM and the dissolved phases with a VARIAN AAS240FS instrument. Minor and trace element (V, Cr, Mn, Co, Ni, Cu, Zn, As, Se, Rb, Sr, Mo, Ag, Cd, Sb, Cs, Ba, and Tl) contents of mineralized SPM and acidified dissolved samples were determined with an inductively coupled plasma quadrupole mass spectrometer (ICP-QMS, X-Series, CCT II & Thermoelectron, France). The control of ICP-QMS precision was done using a standard of river water (SRM 1640a, NIST, USA), and the correction of instrumental drift was based on internal standards deviation (Re, Rh and In). Collision Cell Technology mode using gas input (H_2 (7%) and He (93%)) was used to avoid interferences for elements such as Cr, Fe, Ni, Zn, and As. The standard error for TE concentrations measured in the reference materials (NIST 1940a and SL1 AIEA) was less than 10%. The quantification limits for TE in the dissolved phase were 0.07 µg L^{-1} for Cu, 0.01 µg L^{-1} for Zn, 0.02 µg L^{-1} for Sb and 0.06 µg L^{-1} for Pb.

2.4. Flux calculations

2.4.1. Daily fluxes for each subcatchment and contribution of the downstream subcatchment $Viry_{sub}$

The fluxes of trace elements exported by the Orge River were calculated based on Eqn 1 and 2.

$$\Phi_{part.,I,S} = [TE]_{part.I,S} \times [SPM]_{I,S} \times Q_{river,IS} \quad (1)$$

$$\Phi_{diss.I,S} = [TE]_{diss,I,S} \times Q_{river,IS} \quad (2)$$

where $\Phi_{part,I,S}$ and $\Phi_{diss,I,S}$ are the daily exports of the particulate and dissolved phases respectively for campaign *I* in g d^{-1} at site *S*, $[TE]_{part.I,S}$ is the concentration of TE in g t^{-1} in the suspended solids measured during campaign *I* for site *S*, $[TE]_{diss,I,S}$ is the TE concentration in the dissolved phase in g m^{-3} measured during campaign *I* for site *S*, $[SPM]_{I,S}$ is the total concentration of suspended solids in t m^{-3} measured during campaign *I* for site *S*, and $Q_{river,I,S}$ is the mean water flow rate for site *S* during campaign *I* in m^{-3} d^{-1}. The fluxes were estimated using the median values of $[TE]_{part,I,S}$ (n = 3), $[SPM]_{I,S}$ (n = 4) and $[TE]_{diss,I,S}$ (n = 2). The uncertainties of the TE fluxes were estimated using the standard deviation of $[TE]_{part,I,S}$ and $[TE]_{diss,I,S}$ (i.e., $SD_{ET,part,I,S}$ and $SD_{ET,diss,I,S}$ (in %)) applied respectively to $\Phi_{part,I,S}$ and $\Phi_{diss,I,S}$.

The fluxes calculated at the Egly and Yvette sites corresponded to the exports from the upper portions of the Orge River catchment. By calculation of the difference with the TE exported at the outlet of the entire catchment (i.e., Viry site), we were able to calculate the contribution of the $Viry_{sub}$ subcatchment (i.e., $Contrib_{Viry\ sub}$ in %; Eqn 3 and 4) to the total export of the Orge catchment for the particulate and dissolved phases in each campaign *I*:

$$\text{Contrib}_{part.,I,Viry\ sub} = \frac{\Phi_{part.,I,Viry} - (\Phi_{part.,I,Egly} + \Phi_{part.,I,Yvette})}{\Phi_{part.,I,Viry}} \quad (3)$$

$$\text{Contrib}_{diss.,I,Viry\ sub} = \frac{\Phi_{diss.,I,Viry} - (\Phi_{diss.,I,Egly} + \Phi_{diss.,I,Yvette})}{\Phi_{diss.,I,Viry}} \quad (4)$$

2.4.2. Annual riverine exports of trace element and sediments

The mean annual exports of particulate and dissolved TE were calculated using the following equations (Eqn 6 and 7) based on data for each type of hydrological conditions (i.e., low, average, high water flow periods and the extreme flood of June 2016), as described above (Section 2.2).

$$\Phi_{part,S} = \sum_{i=1}^{365} ([TE]_{part,c,S} \times [SPM]_{c,S} \times Q_{i,c,S}) \quad (6)$$

$$\Phi_{diss,S} = \sum_{i=1}^{365} ([TE]_{diss,c,S} \times Q_{i,c,S}) \quad (7)$$

The annual TE fluxes exported with the particulate phase (i.e. $\Phi_{part,S}$) and the dissolved phase (i.e. $\Phi_{diss,S}$) in g $year^{-1}$ at each site S were estimated as the sum of the daily fluxes calculated for each *i* day in g d^{-1}. Those daily fluxes

were estimated using the median values of $[TE]_{part,c,S}$ in g t^{-1}, $[SPM]_{c,S}$ in t m^{-3} and $[TE]_{diss,c,S}$ in g m^{-3} measured during the campaigns associated with each water flow class *c* (defined in Section 2.2). The daily water flow $Q_{i,c,S}$ in m^3 d^{-1} was continuously recorded by automatic flowmeters located near each sampling site. Trace element exports during the flood of June 2016 (from 05/29/2016 to 06/10/2016), were calculated using [SPM], $[TE]_{diss}$ and $[TE]_{part}$ measured at each site on 06/06/2016.

The uncertainties of the TE annual fluxes were estimated using the standard deviations ($SD_{TE,part,c,S}$ and $SD_{TE,diss,c,S}$ in %) of $[TE]_{part,c,S}$ and $[TE]_{diss,c,S}$ for each water flow class *c* and site *S*. These standard deviations were applied to the daily TE fluxes $\Phi_{part,i,S}$ and $\Phi_{part,i,S}$ (in g d^{-1}) to finally estimate the annual flux uncertainties $SD_{\Phi part,S}$ and $SD_{\Phi diss,S}$ in kg y^{-1} (Eqn 5 and 6).

$$SD_{\Phi part,S} = \sum_{i=1}^{365}(SD_{TE,part,c,S} \times \Phi_{part,i,S}) \quad (8)$$

$$SD_{\Phi diss,S} = \sum_{i=1}^{365}(SD_{TE,diss,c,S} \times \Phi_{diss,i,S}) \quad (9)$$

The sediment fluxes at each site *S*, $\Phi_{SY,S}$ in t y^{-1} were estimated using Eqn 5:

$$\Phi_{SY,S} = \sum_{i=1}^{365}([SPM]_{c,S} \times Q_{i,c,S}) \quad (10)$$

where $[SPM]_{c,S}$ is the concentration of SPM in t m^{-3} at each site *S* for each water flow class *c*, and $Q_{i,c,S}$ is the daily water flow in m^3 d^{-1}. The uncertainties were estimated based on the standard deviation of $[SPM]_{c,S}$ using equation 11:

$$SD_{\Phi SY,S} = \sum_{i=1}^{365}(SD_{SPM,c,S} \times \Phi_{SY,i,S}) \quad (11)$$

2.4.3. Specific fluxes

From the annual particulate TE fluxes calculated using Eqn 6 and the sediment yields using Eqn 10, the specific fluxes of TE ($FS_{TE,S}$) and the specific sediment yield ($FS_{SPM,S}$) were estimated using the drainage area for each subcatchment and used in the following equations (Eqn 12 and 13):

$$FS_{TE,S} = \frac{(\Phi_{TE\,part,S})}{S_{DC,S}} \quad (12)$$

$$FS_{SPM,S} = \frac{(\Phi_{SY,S})}{S_{DC,S}} \quad (13)$$

Therefore, at each site S, the specific particulate TE flux in g km^{-2} y^{-1} and the specific sediment fluxes in t km^{-2} y^{-1} were calculated using the respective annual particulate TE export ($\Phi_{TE,part,S}$) in g y^{-1} and the sediment fluxes ($\Phi_{SY,S}$) in t y^{-1} with the surface area drained at site S $S_{DC,S}$ in km^2. The calculations for the Viry site were considered to correspond to the total of particulate TE exported by the entire catchment. The uncertainties of $FS_{TE,S}$ and $FS_{SPM,S}$ were calculated using equations 12 and 13, with $SD_{\Phi part,S}$ and $SD_{\Phi SY,S}$ respectively replacing $FS_{TE,S}$ and $FS_{SPM,S}$.

3. Results and discussion

3.1. Trace element variations in the water column in response to hydrological changes under urban pressure

Identifying the sources of trace element contamination of the Orge River suspended particulate matter was the objective of a previous study (Froger et al. 2018). In brief, concentrations ranged from 20 to 661 mg kg^{-1} for Cu, from 34 to 980 mg kg^{-1} for Zn, from 0.98 to 4.36 mg kg^{-1} for Sb and from 29 to 151 mg kg^{-1} for Pb, with those concentrations similar to the values found in the Seine River sediments (Le Pape et al. 2012). In this first study, the clear increase in TE enrichment factors in SPM from Dourdan to Viry (Fig 1, Table S2) demonstrated trace element contamination increasing with the densification of urban areas. In addition, lead stable isotopes composition demonstrated the role of road deposited sediments as an important source of particulate TE to the river system.

The dissolved trace elements concentrations shown in Fig 2 ranged from 0.7 to 4.8 µg L^{-1} for Cu, from 0.6 to 38.5 µg L^{-1} for Zn, from 0.1 to 3 µg L^{-1} for Sb and from 0.01 to 0.54 µg L^{-1} for Pb. The ranges of TE concentrations in the dissolved compartment was similar to those found in previous measurements in the Orge River (Le Pape et al. 2012), and they remained below the target values of European guidelines (The European Parliament and the Council of the European Union, 2013). Similar ranges of TE concentrations in dissolved form were observed in other rivers draining urban areas such as the Elbe River (Weigold and Baborowski 2009), or industrialized rivers such as the Lot River (Audry et al. 2004) or the Humber catchment in the UK (Neal et al. 1996). Slightly lower concentrations were measured in the Seine River downstream of Paris City (Priadi et al. 2011), which demonstrates that the Orge River contamination in the dissolved phase is particularly high.

The concentration of dissolved Cu, Zn and Pb increased significantly with the urbanization gradient in the downstream direction (Fig 2, Kruskal-Wallis test, $\alpha = 0.05$). The rise in those dissolved TE concentrations could not be explained by physico-chemical parameters considering the absence of variations in pH and ionic strength between sites (see Fig S3 in the SI). Consequently, anthropogenic activities were considered as a significant source of dissolved TE in the Orge River. and this finding is supported by Le Pape et al. (2014) study that identified point-based urban releases as a significant source of Zn in the Orge River. This was also observed at Egly, by the high Zn concentrations measured in the discharge of untreated wastewater (i.e., $E_{discharge}$; Fig 2). Significant Cu concentrations in the $E_{discharge}$ samples also suggest untreated wastewater releases as a potential source of Cu in the river, as also observed in the Garonne River, where wastewater treatment plants were responsible for 20% of the dissolved Cu inputs (Petit et al. 2013). Those hypotheses of untreated wastewater and runoff water origin for Cu and Zn were supported by the correlation of Cu and Zn dissolved concentrations with the flow rate only for the downstream sites Egly, Yvette and Viry impacted by urbanization (Fig S4 in the supp mat) and not for the upstream site Dourdan. Given the homogeneous geology across the entire catchment in downstream direction (Fig S5), a natural origin of those TE in the river could be ruled out.

With respect to the increase of dissolved Pb with the urbanization gradient, the lower concentrations measured in $E_{discharge}$ led us to rule out the hypothesis that untreated wastewaters might be a major source of Pb. Two hypotheses could explain this increase of Pb in the dissolved compartment: i) the presence of contaminated colloids under 0.45 µm (i.e., porosity of the filter), and ii) desorption of anthropogenic Pb from contaminated particles as anthropogenic lead was identified as more mobile (Kumar et al. 2013). In contrast to the trends observed for Cu, Zn and Pb, the Sb concentrations remained stable across the entire catchment and indicated the absence of significant inputs of dissolved Sb from urban areas therefore suggesting a natural origin of dissolved Sb.

Trace element partitioning (see Table S4 in the SI) between dissolved and particulate phases showed variations between campaigns depending on TE with no specific trend in downstream direction. Dissolved Cu accounted for 52 ± 22% with variations from 9 to 82% (min-max), and dissolved Zn for 49 ± 22% varying from 5 to 83 %, . Most of the Sb was carried by the dissolved phase with a median value of 91 ± 9% of dissolved Sb and variations from 0.3 to 24% of particulate Sb. In contrast, 80 to 99.5% of the Pb was carried by particles with a median value of 94%. These observations are in agreement with those reported in the literature for major rivers (Davide et al. 2003; Rouxel et al. 2003; Audry et al. 2004) and for the Orge River (Le Pape et al. 2012). Differences of partitioning between campaigns were statistically verified (i.e. Kruskal-Wallis test, *p-value* < 0.05), with similar trends for Cu, Pb showing their highest proportion in the particulate phase during the campaigns conducted in

September 2015, January 2016 and August 2016. The proportion of particulate Zn and Sb reached their respective highest values in September 2015 and January 2016 for Zn and in January and June 2016 for Sb. Those trends could be explained by higher SPM concentrations at all sites in September 2015, June 2016, August 2016 and January 2016, with respectively 45.5 mg L^{-1}, 28.2 mg L^{-1}, 26.1 mg L^{-1} and 17.1 mg L^{-1} compared to the concentrations measured in April and November 2016 amounting to 11.5 mg L^{-1} and 6.3 mg L^{-1}. Those results suggest SPM concentration providing the main driver of TE partition in the water column.

3.2. Temporal variations of trace element fluxes

3.2.1. Daily fluxes of dissolved trace elements

The daily fluxes of dissolved trace elements are shown in Fig 3. The highest exports were found during the high water levels of September 2015, with Cu, Zn, Sb and Pb fluxes respectively reaching 1700, 8000, 900 and 120 g d^{-1} (Fig 3). However, exports of dissolved Sb and Pb during the high water levels that occurred in April 2016 were lower than those observed in September 2015 despite similar river discharges. The major difference between those two campaigns was the timing selected because samples from September 2015 were collected during the peak flow with higher SPM concentrations in the river (42 mg L^{-1}, 144 mg L^{-1} and 49 mg L^{-1} at the Egly, Yvette and Viry sites, respectively) compared with the sampling of April 2016 conducted during the decreasing period of the flood with lower SPM concentrations (12 mg L^{-1}, 14 mg L^{-1} and 10 mg L^{-1}, respectively, at the same sites). Higher TE exports during the September 2015 sampling conducted during the peak flow might be explained by a significant load of urban runoff contaminants at the beginning of the flood, also referred to as the "first flush effect" (Lee et al. 2005; Barco et al. 2008). As the April 2016 sampling campaign was conducted after the peak flow, those urban contaminants would have already been exported explaining the lower TE exports during this high waters campaign. Despite the fact that the catchment surface drained at Egly site is about 3 times the surface drained at Yvette site (i.e. 480 km^2 for Egly and 180 km^2 for Yvette), dissolved TE fluxes were similar. Those similar fluxes could not be explained by water flow rates as Egly water flow was twice the rate at Yvette site during all campaigns. Consequently, the Yvette River appears to be under higher anthropogenic pressure than the Orge River at Egly with larger releases of dissolved TE contaminants given the resulting fluxes, which corresponds to the higher proportion of urban areas, found at this particular site.

In addition, variations of daily fluxes at the outlet between the different hydrological periods (i.e. high flow, average flow and low flow periods) appeared not to be directly proportional to the increase of the water flow rates.

Between low and high flow periods, water flow rates were multiplied by 4 whereas the daily fluxes of Cu, Zn Sb and Pb were multiplied respectively by 6, 10, 6 and 5. Conversely, the difference between average and low flow periods remained in the same range as water flow rate differences. Therefore, drastic increases of water flow rates in the Orge catchment result in higher contamination levels across the water column, especially in dissolved Zn.

The results of inputs from $Viry_{sub}$ (Table 1) showed that the downstream urban subcatchment of $Viry_{sub}$ contributed 50% of the total dissolved Cu and Pb fluxes exported by the catchment and up to 75% of the total dissolved Zn flux. The fluxes of dissolved TE from Viry subcatchment were much higher than its respective contribution to the water discharge at the outlet, ranging from 15 to 23% (Table 1). $Viry_{sub}$ supplied the majority of dissolved Cu, Zn and Pb fluxes transiting the Orge River during all campaigns, the main hypothesis being the discharge of untreated wastewaters and runoff into the river, supplying dissolved TE as well as highly contaminated particles with more reactive TE-bearing phases. The stability of the mean $Viry_{sub}$ contributions to the dissolved Cu and Pb exports, regardless of hydrological conditions, suggests a continuous supply of diffuse TE pollutions from urban areas (Estebe et al. 1998; Sabin et al. 2005). In contrast, the larger variations of the $Viry_{sub}$ contribution to dissolved Zn exports were likely explained by the occurrence of point-based sources such as untreated wastewater inputs specifically enriched in this chemical element (Fig 2; Chen et al. (2009); Le Pape et al. (2012)).

Antimony showed a different behavior than Zn, Cu and Pb. The $Viry_{sub}$ contributions to the total dissolved Sb export were 15% during the September 2015 and August 2016 campaigns, i.e., during high and low flows, respectively, equivalent to its contribution to the river water flow at the outlet (Table 1). In contrast, the contribution of $Viry_{sub}$ to the total dissolved Sb exported reached up to 31%, 42% and 42% in the January, April and November 2016 campaigns, respectively, presenting different hydrological conditions (Table 1). During those three campaigns, continuous urban runoff resulting from frequent rainfall events was identified as the main source of particulate TE delivered to the Orge River SPM (Froger et al. 2018). Consequently, urban runoff might act as a source of dissolved Sb, and possible desorption of Sb from contaminated particles could also contribute to the increasing concentrations in the dissolved phase because road traffic is an important source of this element (Filella 2011; Fujiwara et al. 2011).

3.2.2. Daily fluxes of particulate trace elements

Particulate TE fluxes at the outlet ranged from 111 to 1065 g d^{-1} for Cu, from 248 to 5583 g d^{-1} for Zn, from 3 to 51 g d^{-1} for Sb and from 103 to 1202 g d^{-1} for Pb (Fig 4). The highest fluxes were observed during the September

2015 flood with the highest water flow rate (Fig 4) associated with high SPM concentrations. The lowest fluxes were found during the low flow periods corresponding to the June 2015 campaign for Cu and Pb and to the August 2016 campaign for Zn and Sb. Those results differed from those of Poulier et al. (2019) who calculated the fluxes in the Rhône River catchment showing lower concentrations of Hg and PCB in SPM during flood conditions. Consequently, the behavior of particulate TE in the Orge River catchment likely reflects the widespread contamination of soil and sediments in this early-industrialized catchment.

The contribution of the $Viry_{sub}$ subcatchment to the total TE exported by SPM reached 70% (Table 2) during the average flow periods (i.e., January and November 2016) and the high waters of April 2016. These higher contributions could be attributed to diffuse urban inputs such as urban runoff, in line with the report by Froger et al. (2018) that radionuclide chronometers and lead isotopic compositions identified road deposited sediments as a major source of particulate TE to the river, especially during average flow periods.

3.3. Case of the exceptional flood of June 2016

3.3.1. Fluxes of dissolved and particulate trace elements

The fluxes of particulate and dissolved Cu, Zn, Sb and Pb exported at each sampling site for this flood were calculated and are reported in Table 3. The particulate exports of Cu, Zn, Sb and Pb reached 12, 50, 0.22 and 9 kg d^{-1} and were 10, 10, 4 and 7.5 times higher, respectively, than those fluxes measured during the high water flow period of September 2015 (Table 3). Zinc, Sb and Pb exports from the Egly subcatchment were in the same range as the fluxes estimated for the entire catchment (i.e., calculated at the Viry site) (Table 3). This observation could be explained by the high TE concentrations measured in Egly SPM during this event, which reached 666 mg kg^{-1} for Zn and 120 mg kg^{-1} for Pb when the maximum concentrations for the other campaigns were 645 and 74 mg kg^{-1}, respectively (Table S1). Therefore, this extreme event resulted in a drastic increase in the export of particulate TE at the Egly site, which could be considered as the outlet of the main agricultural area in the upstream portion of the Orge River catchment. During the time of the flood, the cumulative effect of highly contaminated particles and high SPM content in the water column resulted in a maximum TE export at the Egly site (Ollivier et al. 2011).

The fluxes of dissolved TE reached 4.6 kg d^{-1} for Cu, 11.9 kg d^{-1} for Zn, 0.47 kg d^{-1} for Sb and 0.41 kg d^{-1} for Pb on the 6th of June 2016. Those exports were 3, 3.5 and 1.5 times higher than the respective fluxes of Cu, Pb and Zn exported during the high waters of September 2015 (Fig 3). In contrast, Sb exports during the flood of June 2016 were lower than those during the high water flow period of September 2015, suggesting a dilution of dissolved Sb during the exceptional June 2016 flood. From the different dissolved TE fluxes at the outlet (Viry)

and the sampling sites of Yvette and Egly, the contributions of each subcatchment (i.e., Egly, Yvette and $Viry_{sub}$) were estimated (Fig 5). The contributions of the three subcatchments differed depending on the TE considered. Dissolved Cu exported by each subcatchment was equivalent to its respective contribution to the total export of water (i.e., waterflow distribution, Fig 5). This result could be explained by the homogeneous concentrations of dissolved Cu over the catchment, indicating the absence of additional inputs from one specific subcatchment. In contrast, the contribution of the $Viry_{sub}$ subcatchment to the outlet daily fluxes of dissolved Zn and Pb reached 40% and 50%, respectively, underlining the supply of additional inputs, such as building siding, which has been identified as the highest source of Pb and Zn in urban runoff (Davis et al. 2001). Finally, the higher contribution of Sb from the Yvette subcatchment (Fig 5) could be explained by the presence of gypsum marls in the Yvette riverbed (Vernoux et al. 1999), which could contain Sb because it is a widely diffused element in geological material containing sulfates (Boyle and Jonasson 1984). During the flood, this material might have been drained by groundwater releasing Sb in the river. Isotopic tools (i.e., $\delta^{66}Zn$, $\delta^{123}Sb$, $^{206}Pb/^{207}Pb$) could be of help in estimating the contribution of each source to the dissolved fluxes of Zn, Pb and Sb (Kumar et al. 2009; Chen et al. 2009; Resongles et al. 2015).

3.3.2. Contribution of June 2016 flood to the yearly export of trace elements

The total exports of TE during the June 2016 flood (from the 29th of May to the 10th of June 2016) were calculated and reported in Table 4. The estimated fluxes were subsequently compared with the TE exported during the entire year in 2016 (see Section 2.4.2.1 for detailed calculations) and are reported in Table 4.

Fifty to sixty percent of the annual particulate TE loads of 2016 was exported during the flood of June 2016, which is lower than the amount estimated in previous studies showing that up to 90% of the annual fluxes could be exported during flood events (Coynel et al. 2009; Ollivier et al. 2011).

During the flood of June 2016, higher TE concentrations in SPM were observed only at the Egly site (Section 3.3.1). In contrast, SPM collected at the Orge catchment outlet (i.e., the Viry site) showed TE concentrations of 108, 472, 2.1 and 84 mg kg^{-1} for Cu, Zn, Sb and Pb, respectively. These concentrations were similar to the median values obtained in the Viry SPM during all other campaigns with 85 mg kg^{-1} for Cu, 408 mg kg^{-1} for Zn, 3.2 mg kg^{-1} for Sb and 88 mg kg^{-1} for Pb. Those results explain the correspondence of the contribution of the flood to the annual particulate TE exports (50-60%) with its contribution to the annual SPM export (56%) (Table 4 Le Gall et al. (2018) analysed the flood sediments deposited during the exceptional June 2016 flood in the Seine River basin and showed that sediment remobilization was the major source of particles transported during the flood in the Orge

catchment. However, conversely to the downstream part of the Seine River catchment showing enrichment factors in flood sediment deposits lower than values reported during the last several decades (Le Gall et al. 2018), enrichment factors in the Orge River SPM during the flood were equivalent to EF observed during the other campaigns (see Table S2). Those results demonstrated the widespread contamination of the Orge catchment as a result of long-term pollution from human activities in the area (Thévenot et al. 2007; Le Cloarec et al. 2011). In addition to TE originating from sediment remobilization, anthropogenic TE deposited on urban surfaces such as roads, roofs and sewer networks (Percot et al. 2016) could also contribute to the load of contaminated SPM delivered to the river during the flood of June 2016.

The contribution of the flood of June 2016 to the annual dissolved TE fluxes reached up to 21% and 27% for Cu and Pb, respectively, and 15% and 7% for Zn and Sb. Fourteen percent of the annual water flow was exported during the flood, indicating that additional inputs of Cu and Pb were observed during this event. These inputs could be due to runoff on surfaces that are usually not washed off during less intensive rainfall events, thus supplying contaminated particles to the river. Moreover, a higher concentration of contaminated colloids under 0.45 µm could increase TE concentrations in the dissolved fraction of the water column. In contrast to Cu and Pb, a dilution effect was observed for Sb supporting a geogenic origin for dissolved Sb. Finally, concentrations of Zn in the dissolved phase were not affected by June 2016 flood because its contribution of 15% to the annual Zn fluxes matched its contribution to the annual water flow of 14%. Overall, the contribution of the June 2016 flood to the export of dissolved TE followed the affinity to the particulate phase in the order Pb>Cu>Zn>Sb.

Finally, the major flood event that occurred in June 2016 contributed to 9, 37, 40 and 53% of the total annual exports for Sb, Zn, Cu and Pb, respectively. These results underlined the specific behavior of such catchments with highly urbanized surfaces downstream, where the export of TE is significant during regular hydrological conditions and not only during flood events (Froger et al. 2018). These results also underline that Sb behaves quite differently than other urban elements probably because Sb sources are both natural for dissolved Sb and anthropogenic for particulate Sb.

3.4. Annual fluxes

The previous results demonstrated the homogenous release of all four contaminants (Cu, Zn, Sb and Pb) associated with the particulate phase from urban areas in the Orge catchment. Conversely, heterogeneous dissolved TE inputs from urban areas were shown, depending on the TE considered, with wide variations in TE concentrations between campaigns (Fig 2). Consequently, particulate TE was identified as a reliable indicator to represent global TE

contamination of the catchment. Fluxes of particulate trace elements were estimated for the years 2015 and 2016, and the interannual mean value was calculated. Specific TE fluxes and specific sediment yields were estimated for a compilation of studies selected based on the catchment characteristics (i.e., urban/rural) and the available data that allowed specific flux calculations (Table 5).

The annual specific loads of Cu, Zn, Sb and Pb found in the current research were 232, 1070, 5.7 and 197 g $km^{-2}y^{-1}$, respectively, and these values are lower than most of the fluxes reported in the literature except for the Thames River and the Colorado River (Table 5). The lower fluxes found in the Orge, Thames and Colorado River catchments could be attributed to their specific sediment yields of respectively 2.3, 5.6 and 1 t km^{-2} y^{-1}, values that are 10 to 100 times lower than those reported in the other catchments.

We developed a new tool based on the ratio of specific particulate TE fluxes (i.e., FS_{TE}) and specific sediment yield (i.e., FS_{SPM}) to evaluate and compare the level of anthropogenic pressure undergone by catchments having different geographical and geological features (e.g., propensity to erosion) presented in Table 5. Consequently, the FS_{TE}/FS_{SPM} ratio integrates the catchment parameters such as the solid fluxes and the drained surface which site-to-site variation may precludes the observation of particulate contaminant flux variations.

In the Orge River catchment, the FS_{TE}/FS_{SPM} ratio increased in the downstream direction following the urbanization gradient. The trace element specific fluxes of $Viry_{sub}$ appeared to be similar to the fluxes estimated for the entire catchment (i.e., at Viry station) despite the lower specific sediment yield calculated for the $Viry_{sub}$ subcatchment (i.e., FS_{SPM} of 0.2 t km^{-2} y^{-1} for $Viry_{sub}$ compared with 2.3 t km^{-2} y^{-1} for the entire catchment) (Table 4). This result indicates a lower amount of particles supplied by urban areas compared with rural areas and resulted in high FS_{TE}/FS_{SPM} ratios for the most urban subcatchments, especially for Cu, Zn and Sb, which respectively reached 707, 747 and 18 g t^{-1}, values that are 7, 1.6 and 9 times the ratios of 101, 465 and 2.5 g t^{-1} found for the entire catchment. Conversely, the Pb ratios of 114 g t^{-1} found for $Viry_{sub}$ appeared to fall in the same range as the entire catchment FS_{TE}/FS_{SPM} ratios. Therefore, the urban areas in the Orge River catchment were a significant source of particulate Cu and Sb to the river.

In comparing with other catchments, catchments that drain large urban areas such as the Seine River (France), and the Atlanta and San Francisco (USA) catchments, regardless of their drainage area, showed FS_{TE}/FS_{SPM} ratios for Cu, Zn, and Pb of approximately 100, 500 and 100 g t^{-1}, respectively (Table 5). The highest values were found in the Seine River catchment, which is known for its long-term history of sediment contamination by TE (Meybeck et al. 2007). The similar values of the FS_{ET}/FS_{SPM} ratios for the Orge River catchment and the urban catchments

of Atlanta and San Francisco underlined the homogeneity of contamination in catchments that present a high proportion of urban surfaces despite their various characteristics and sediment dynamics. Despite its lower urban cover, the Garonne River catchment showed FS_{TE}/FS_{SPM} ratios similar to those found in the urban catchments of Atlanta and San Francisco. These results can be explained by the drainage of Bordeaux city at the outlet and the contamination of the Lot sub-catchment by mining and industrial activities (Audry et al. 2004). In catchments with less urban cover, the Cu, Zn and Pb FS_{TE}/FS_{SPM} ratios are under 50, 300 and 60, respectively, with the Rhône River presenting the highest values of the ratio, which reflects the presence of anthropogenic releases from cities such as Lyon, Valence of Arles in the catchment (Ollivier et al. 2011). Finally, these findings confirm that similar to the PAH case, the FS_{TE}/FS_{SPM} ratio is (Froger et al. 2019a) an effective tool that can be used to compare the contamination level of catchments affected by anthropogenic activities.

4. Conclusions

To conclude, management of contaminants at the catchment scale must be based on a deep knowledge of both the sources and the behavior of contaminants in the river across the catchments. However, few studies have quantified the fluxes of contaminants linked to an increase in urban areas at the catchment scale and the response of those urban inputs to hydrological variations. In the current study, the fluxes of particulate Cu, Zn, Sb and Pb were quantified. The contribution of the urban area in the downstream portion of the catchment to the total annual export of particulate trace elements reached 70% during average water flow periods. Dissolved urban inputs remained stable over the different hydrological conditions, with a contribution greater than 50% for Cu, Zn and Pb and between 15 and 40% for Sb, suggesting that urban sources continuously supplied contaminants. The exceptional flood of June 2016 exported 50 to 60% of the annual particulate TE load, and the particles transported were identified as remobilized sediments, underlining the long-term contamination of the catchment. This observation suggests the need to conduct longitudinal studies that integrate all hydrological conditions when assessing river contamination, especially in an urban context. Finally, the ratios of specific fluxes underlined the similarities in the contaminant exports of catchments that drain mostly urban areas and might be used to compare the levels of anthropogenic pressure between urbanized catchments around the world. An assessment of the catchment state of contamination using the ratio of specific fluxes could be performed to support policy implementations and local actions to reduce contaminant releases.

Acknowledgements

This research was financially supported by Paris-Sud University (PhD grant), the ”Initiative de Recherche Stratégique” ACE-ICSEN funded by the University Paris-Saclay and the Seine River research program PIREN-Seine.

Compliance with Ethical Standards

We declare that the current research respects the ethical standards of the journal, with no potential conflicts of interest. and did not involve neither Human Participants nor animals.

References

Adachi K, Tainosho Y (2004) Characterization of heavy metal particles embedded in tire dust. Environ Int 30:1009–1017. https://doi.org/10.1016/j.envint.2004.04.004

Adamiec E, Jarosz-Krzemińska E, Wieszała R (2016) Heavy metals from non-exhaust vehicle emissions in urban and motorway road dusts. Environ Monit Assess 188:1–11. https://doi.org/10.1007/s10661-016-5377-1

Audry S, Schafer J, Blanc G, et al (2004) Anthropogenic components of heavy metal (Cd, Zn, Cu, Pb) budgets in the Lot-Garonne fluvial system (France). Appl Geochemistry 19:769–786. https://doi.org/10.1016/j.apgeochem.2003.10.002

Ayrault S, Priadi CR, Pape P Le, Bonté P (2013) Occurrence, sources and pathways of antimony and silver in an urban catchment. In: Rauch S, Morrison G, Norra S, Schleicher N (eds) Urban Environment. Springer Netherlands, Dordrecht, pp 425–435

Ayrault S, Roy-Barman M, Le Cloarec MF, et al (2012) Lead contamination of the Seine River, France: Geochemical implications of a historical perspective. Chemosphere 87:902–910. https://doi.org/10.1016/j.chemosphere.2012.01.043

Barco J, Papiri S, Stenstrom MK (2008) First flush in a combined sewer system. Chemosphere 71:827–833. https://doi.org/10.1016/j.chemosphere.2007.11.049

Becouze-Lareure C, Dembélé A, Coquery M, et al (2016) Source characterisation and loads of metals and pesticides in urban wet weather discharges. Urban Water J 13:600–617. https://doi.org/10.1080/1573062X.2015.1011670

Boyle RW, Jonasson IR (1984) The geochemistry of antimony and its use as an indicator element in geochemical prospecting. J Geochemical Explor 20:223–302. https://doi.org/10.1016/0375-6742(84)90071-2

Brown JN, Peake BM (2006) Sources of heavy metals and polycyclic aromatic hydrocarbons in urban stormwater runoff. Sci Total Environ 359:145–155. https://doi.org/10.1016/j.scitotenv.2005.05.016

Charters FJ, Cochrane TA, O'Sullivan AD (2016) Untreated runoff quality from roof and road surfaces in a low intensity rainfall climate. Sci Total Environ 550:265–272. https://doi.org/10.1016/j.scitotenv.2016.01.093

Chen J, Gaillardet J, Louvat P, Huon S (2009) Zn isotopes in the suspended load of the Seine River, France: Isotopic variations and source determination. Geochim Cosmochim Acta 73:4060–4076. https://doi.org/10.1016/J.GCA.2009.04.017

Coynel A, Blanc G, Marache A, et al (2009) Assessment of metal contamination in a small mining- and smelting-affected watershed: high resolution monitoring coupled with spatial analysis by GIS. J Environ Monit 11:962–976. https://doi.org/10.1039/b818671e

Davide V, Pardos M, Diserens J, et al (2003) Characterisation of bed sediments and suspension of the river Po (Italy) during normal and high flow conditions. Water Res 37:2847–2864. https://doi.org/10.1016/S0043-1354(03)00133-7

Davis AP, Shokouhian M, Ni S (2001) Loading estimates of lead, copper, cadmium, and zinc in urban runoff from specific sources. Chemosphere 44:997–1009. https://doi.org/10.1016/S0045-6535(00)00561-0

Estebe A, Mouchel JM, Thevenot DR (1998) Urban runoff impacts on particulate metal concentrations. Water Air Soil Pollut 108:83–50. https://doi.org/10.1023/A:1005064307862

Filella M (2011) Antimony interactions with heterogeneous complexants in waters, sediments and soils: A review of data obtained in bulk samples. https://doi.org/10.1016/j.earscirev.2011.04.002

Froger C, Ayrault S, Evrard O, et al (2018) Tracing the sources of suspended sediment and particle-bound trace metal elements in an urban catchment coupling elemental and isotopic geochemistry, and fallout radionuclides. Environ Sci Pollut Res 25:28667–28681. https://doi.org/10.1007/s11356-018-2892-3

Froger C, Ayrault S, Gasperi J, et al (2019a) Innovative combination of tracing methods to differentiate between legacy and contemporary PAH sources in the atmosphere-soil-river continuum in an urban catchment (Orge River, France). Sci Total Environ 669:448–458. https://doi.org/10.1016/j.scitotenv.2019.03.150

Froger C, Quantin C, Gasperi J, et al (2019b) Impact of urban pressure on the spatial and temporal dynamics of PAH fluxes in an urban tributary of the Seine River (France). Chemosphere 219:1002–1013. https://doi.org/10.1016/j.chemosphere.2018.12.088

Fujiwara F, Rebagliati RJ, Marrero J, et al (2011) Antimony as a traffic-related element in size-fractionated road dust samples collected in Buenos Aires. Microchem J 97:62–67. https://doi.org/10.1016/j.microc.2010.05.006

Gateuille D, Evrard O, Lefevre I, et al (2014) Mass balance and decontamination times of Polycyclic Aromatic Hydrocarbons in rural nested catchments of an early industrialized region (Seine River basin, France). Sci Total Environ 470–471:608–617. https://doi.org/10.1016/j.scitotenv.2013.10.009

Hasenmueller EA, Criss RE, Winston WE, Shaughnessy AR (2017) Stream hydrology and geochemistry along a rural to urban land use gradient. Appl Geochemistry 83:136–149. https://doi.org/10.1016/j.apgeochem.2016.12.010

Horowitz AJ (2009) Monitoring suspended sediments and associated chemical constituents in urban environments: Lessons from the city of Atlanta, Georgia, USA water quality monitoring program. J Soils Sediments 9:342–363. https://doi.org/10.1007/s11368-009-0092-y

Horowitz AJ, Elrick KA, Smith JJ (2001) Annual suspended sediment and trace element fluxes in the Mississippi, Columbia, Colorado, and Rio Grande drainage basins. Hydrol Process 15:1169–1207. https://doi.org/10.1002/hyp.209

Hu B, Li J, Bi N, et al (2015) Seasonal variability and flux of particulate trace elements from the Yellow River: Impacts of the anthropogenic flood event. Mar Pollut Bull 91:35–44. https://doi.org/10.1016/j.marpolbul.2014.12.030

Kumar M, Furumai H, Kurisu F, Kasuga I (2013) Tracing source and distribution of heavy metals in road dust, soil and soakaway sediment through speciation and isotopic fingerprinting. Geoderma 211–212:8–17. https://doi.org/10.1016/j.geoderma.2013.07.004

Kumar M, Furumai H, Kurisu F, Kasuga I (2009) Understanding the partitioning processes of mobile lead in soakaway sediments using sequential extraction and isotope analysis. Water Sci Technol 60:2085–2091. https://doi.org/10.2166/wst.2009.512

Lamprea K, Ruban V (2011) Pollutant concentrations and fluxes in both stormwater and wastewater at the outlet of two urban watersheds in Nantes (France). Urban Water J 8:219–231. https://doi.org/10.1080/1573062X.2011.596211

Le Cloarec MF, Bonte PH, Lestel L, et al (2011) Sedimentary record of metal contamination in the Seine River during the last century. Phys Chem Earth 36:515–529. https://doi.org/10.1016/j.pce.2009.02.003

Le Gall M, Ayrault S, Evrard O, et al (2018) Investigating the metal contamination of sediment transported by the

2016 Seine River flood (Paris, France). Environ Pollut 240:125–139. https://doi.org/10.1016/j.envpol.2018.04.082

Le Pape P, Ayrault S, Michelot J-L, et al (2013) Building an isotopic hydrogeochemical indicator of anthropogenic pressure on urban rivers. Chem Geol 344:63–72. https://doi.org/10.1016/j.chemgeo.2013.02.018

Le Pape P, Ayrault S, Quantin C (2012) Trace element behavior and partition versus urbanization gradient in an urban river (Orge River, France). J Hydrol 472–473:99–110. https://doi.org/10.1016/j.jhydrol.2012.09.042

Le Pape P, Quantin C, Morin G, et al (2014) Zinc speciation in the suspended particulate matter of an urban river (Orge, France): influence of seasonality and urbanization gradient. Environ Sci Technol 48:11901–11909. https://doi.org/10.1021/es500680x

Lee BC, Matsui S, Shimizu Y, Matsuda T (2005) Characterizations of the first flush in storm water runoff from an urban roadway. Environ Technol 26:773–782. https://doi.org/10.1080/09593332608618508

McKee LJ, Gilbreath AN (2015) Concentrations and loads of suspended sediment and trace element pollutants in a small semi-arid urban tributary, San Francisco Bay, California. Environ Monit Assess 187:. https://doi.org/10.1007/s10661-015-4710-4

Meybeck M, Lestel L, Bonté P, et al (2007) Historical perspective of heavy metals contamination (Cd, Cr, Cu, Hg, Pb, Zn) in the Seine River basin (France) following a DPSIR approach (1950-2005). Sci Total Environ 375:204–231. https://doi.org/10.1016/j.scitotenv.2006.12.017

Navratil O, Evrard O, Esteves M, et al (2012) Core-derived historical records of suspended sediment origin in a mesoscale mountainous catchment: the River Bléone, French Alps. J Soils Sediments 12:1463–1478. https://doi.org/10.1007/s11368-012-0565-2

Neal C, Davies H (2003) Water quality fluxes for eastern UK rivers entering the North Sea: a summary of information from the Land Ocean Interaction Study (LOIS). Sci Total Environ 314–316:821–882. https://doi.org/10.1016/S0048-9697(03)00086-X

Neal C, Smith CJ, Jeffery HA, et al (1996) Trace element concentrations in the major rivers entering the Humber estuary, NE England. J Hydrol 182:37–64. https://doi.org/10.1016/0022-1694(95)02940-0

Némery J, Mano V, Coynel A, et al (2013) Carbon and suspended sediment transport in an impounded alpine river (Isère, France). Hydrol Process 27:2498–2508. https://doi.org/10.1002/hyp.9387

Nriagu JO (1996) A History of Global Metal Pollution. Science (80-) 272:223–0. https://doi.org/10.1126/science.272.5259.223

Ollivier P, Radakovitch O, Hamelin B (2011) Major and trace element partition and fluxes in the Rhône River. Chem Geol 285:15–31. https://doi.org/10.1016/j.chemgeo.2011.02.011

Percot S, Ruban V, Roupsard P, et al (2016) A new method for assessing the contribution of atmospheric deposition to the stormwater runoff metal load in a small urban catchment. Water Air Soil Pollut 227:1–13. https://doi.org/10.1007/s11270-016-2794-2

Petit JCJ, Schäfer J, Coynel A, et al (2013) Anthropogenic sources and biogeochemical reactivity of particulate and dissolved Cu isotopes in the turbidity gradient of the Garonne River (France). Chem Geol 359:125–135. https://doi.org/10.1016/j.chemgeo.2013.09.019

Pistocchi A, Dorati C, Aloe A, et al (2019) River pollution by priority chemical substances under the Water Framework Directive: A provisional pan-European assessment. Sci Total Environ 662:434–445. https://doi.org/10.1016/j.scitotenv.2018.12.354

Poulier G, Launay M, Le Bescond C, et al (2019) Combining flux monitoring and data reconstruction to establish annual budgets of suspended particulate matter, mercury and PCB in the Rhône River from Lake Geneva to the Mediterranean Sea. Sci Total Environ 658:457–473. https://doi.org/10.1016/j.scitotenv.2018.12.075

Priadi C, Bourgeault A, Ayrault S, et al (2011) Spatio-temporal variability of solid, total dissolved and labile metal: passive vs. discrete sampling evaluation in river metal monitoring. J Environ Monit 13:1470. https://doi.org/10.1039/c0em00713g

Resongles E, Freydier R, Casiot C, et al (2015) Antimony isotopic composition in river waters affected by ancient mining activity. Talanta 144:851–861. https://doi.org/10.1016/j.talanta.2015.07.013

Revitt DM, Ellis JB (2016) Urban surface water pollution problems arising from misconnections. Sci Total Environ 551–552:163–174. https://doi.org/10.1016/j.scitotenv.2016.01.198

Rouxel O, Ludden J, Fouquet Y (2003) Antimony isotope variations in natural systems and implications for their use as geochemical tracers. Chem Geol 200:25–40. https://doi.org/10.1016/S0009-2541(03)00121-9

Sabin LD, Jeong HL, Stolzenbach KD, Schiff KC (2005) Contribution of trace metals from atmospheric deposition to stormwater runoff in a small impervious urban catchment. Water Res 39:3929–3937.

https://doi.org/10.1016/j.watres.2005.07.003

SAGE Orge-Yvette (2011) Actualisation de l'état des lieux et du diagnostic

Schneider V (2005) Apports de l'hydrodynamique et de la géochimie à la caractérisation des nappes de l'Oligocène et de l'Eocène et à la reconnaissance de leurs relations actuelles et passées: origine de la dégradation de la nappe de l'Oligocène (sud-ouest du bassin de Paris. PhD Thesis. Paris-Sud University

The European Parlament and the Council of the European Union (2013) Directives of 12 August 2013 amending Directives 2000/60/EC and 2008/105/EC as regards priority substances in the field of water policy. Off. J. Eur. Union 2013:1–17

Thévenot DR, Moilleron R, Lestel L, et al (2007) Critical budget of metal sources and pathways in the Seine River basin (1994-2003) for Cd, Cr, Cu, Hg, Ni, Pb and Zn. Sci Total Environ 375:180–203. https://doi.org/10.1016/j.scitotenv.2006.12.008

Van Metre P., Mahler B. (2003) The contribution of particles washed from rooftops to contaminant loading to urban streams. Chemosphere 52:1727–1741. https://doi.org/10.1016/S0045-6535(03)00454-5

Van Metre PC, Mesnage V, Laignel B, et al (2008) Origins of sediment-associated contaminants to the Marais Vernier, the Seine Estuary, France. Water Air Soil Pollut 191:331–344. https://doi.org/10.1007/s11270-008-9628-9

Vernoux J, Barbier J, Donsimoni M, et al (1999) Etude hydrogéologique du plateau de Saclay (Essonne), rapport BRGM SGR/IDF R 40840

Weigold F, Baborowski M (2009) Consequences of delayed mixing for quality assessment of river water: Example Mulde-Saale-Elbe. J Hydrol 369:296–304. https://doi.org/10.1016/j.jhydrol.2009.02.039

Zachmann DW, van der Veen A, Friese K (2013) Floodplain lakes as an archive for the metal pollution in the River Elbe (Germany) during the 20th century. Appl Geochemistry 35:14–27. https://doi.org/10.1016/j.apgeochem.2013.05.009

Tables:

Table 1 Contribution of $Viry_{sub}$ to TE export by the dissolved phase together with the contribution of $Viry_{sub}$ to the total water flow (outlet) in %

Contribution of $Viry_{sub}$ to the total dissolved export (%)	**Cu**	**Zn**	**Sb**	**Pb**	**Contribution of $Viry_{sub}$ to the Orge River water flow (%)**
September 2015	48 ± 20	57 ± 33	15 ± 16	58 ± 21	20
January 2016	48 ± 15	75 ± 7	31 ± 3	50 ± 4	15
April 2016	56 ± 11	44 ± 24	42 ± 5	54 ± 6	23
August 2016	57 ± 5	59 ± 12	15 ± 3	45 ± 10	22
November 2016	42 ± 13	65 ± 13	42 ± 4	54 ± 8	18

Table 2 Contributions of $Viry_{sub}$ to the total fluxes of particulate Cu, Zn, Sb and Pb exported by the Orge catchment for the campaigns of January, April and November 2016

Contribution of $Viry_{sub}$ to the total particulate export (%)	**Cu**	**Zn**	**Sb**	**Pb**
January 2016	73 ± 6	75 ± 6	76 ± 4	73 ± 6
April 2016	42 ± 14	33 ± 15	52 ± 9	33 ± 9
November 2016	61 ± 11	53 ± 7	71 ± 3	56 ± 6

Table 3 Daily fluxes at Dourdan, Egly, Yvette and Viry sites on the 6th of June 2016

Daily fluxes	**Particulate phase (kg d^{-1})**	**Dissolved fluxes (kg d^{-1})**	**Flow rate**

	Cu	Zn	Sb	Pb	Cu	Zn	Sb	Pb	$m^3 s^{-1}$
D 06/06/2016	0.3	1.5	0.01	0.3	0.09	0.16	0.01	0.01	0.6
E 06/06/2016	4.2	50.1	0.17	9.1	2.64	4.25	0.18	0.07	9.1
Y 06/06/2016	2.7	11.6	0.03	1.6	1.06	3.26	0.24	0.12	3.1
V 06/06/2016	11.5	50.2	0.22	8.9	4.64	11.90	0.47	0.41	15.2

Table 4 Fluxes of TE exported at the catchment outlet (i.e., Viry site) in kg during the June 2016 flood compared with the fluxes for the entire year 2016

		Cu	**Zn**	**Sb**	**Pb**	**SPM exported**
Fluxes of June 2016 flood (kg)	Particulate	200 ± 27	871 ± 96	4 ± 0.5	155 ± 11	$1846.\ 10^3$ ± 262
	Dissolved	80 ± 24	206 ± 90	8 ± 0.8	7 ± 2	
	Total	280 ± 51	1078 ± 186	12 ± 1.3	162 ± 13	
Fluxes year 2016 (kg)	Particulate	327 ± 53	1514 ± 195	8 ± 1	277 ± 29	3290.10^3 ± 602
	Dissolved	380 ± 101	1378 ± 524	121 ± 10	27 ± 5	
	Total	707 ± 154	2892 ± 719	129 ± 11	303 ± 34	
Contribution of the flood to the total annual export (%)	Particulate	61	58	50	56	56
	Dissolved	21	15	7	27	
	Total	40	37	9	53	

Table 5: Annual specific fluxes of particulate trace elements (FS_{TE}) in g km^{-2} y^{-1} exported at each sampling site of the Orge River and catchments from the literature together with SPM specific fluxes (FS_{SPM}) in t km^{-2} y^{-1} and the ratio of TE specific fluxes and SPM specific fluxes

			FS_{SPM}	**FS_{Cu}**	**FS_{Zn}**	**FS_{Sb}**	**FS_{Pb}**	**Cu**	**Zn**	**Sb**	**Pb**	**References**
		Land use	t km^{-2} y^{-1}	g km^{-2} y^{-1}				Ratio FS_{TE}/FS_{SPM}				
Orge River (France)	Dourdan	Rural	4.4 ± 1.8	277 ±111	1251 ±407	6.1 ±0.6	261 ±16	62	282	1.4	59	This study
	Egly	Rural	2.7 ± 0.4	173 ±41	1289 ±238	5.7 ±0.3	250 ±25	64	476	2.1	92	

	Yvette	Mixed	4.7 ± 0.8	527 ±114	1991 ±354	8.9 ±0.5	339 ±42	113	427	1.9	73	
	Outlet	Mixed/Urban	2.3 ± 0.5	232 ±42	1070 ±148	5.7 ±0.8	197 ±23	101	465	2.5	86	
	$Viry_{sub}$	Urban	0.2 ± 0.02	148 ±36	157 ±34	3.8 ±0.5	24 ±3	707	747	18	114	
Garonne River (France)	Mixed/Industrial		146	14274	101351		12669	98	694	-	87	(Audry et al. 2004)
Rhône River (France)	Mixed		74	4291	17632	210	5101	58	239	3	69	(Ollivier et al. 2011)
Seine River (France)	Urban		10	1298	4869	25*	1352	130	487	2.5	135	(Thévenot et al. 2007) *(Ayrault et al. 2013)
Thames River (UK)	Urban		5.6	330	1200	-	300	59	214	-	54	(Neal and Davies 2003)
Mississippi River (USA)	Rural/Mixed		42	916	4599	47	1000	22	110	1.1	24	(Horowitz et al. 2001)
Columbia river (USA)	Rural/Mixed		57	2775	9626	57	1359	49	170	1.0	24	
Colorado River (USA)	Mixed		1	39	137	3	37	31	108	2.7	29	
Yellow River (China)	Rural/Mixed		198	6242	15980	-	5384	32	81	-	27	(Hu et al. 2015)
Atlanta catchment (USA)	Urban		163	15172	69388	-	13839	93	425	-	85	(Horowitz 2009)
San Francisco catchment (USA)	Urban		32	2800	18000	-	2000	89	571	-	63	(McKee and Gilbreath 2015)

Figure captions:

Fig 1 The Orge River catchment: land use (source: Corine Land Cover), study sites and drained sub-catchment

*Fig 2 Trace element concentrations in µg L^{-1} in the dissolved phase for samples collected in the Orge River and in untreated water discharge collected near the Egly site (Edischarge) for the six sampling campaigns. The data used in the statistical test are included in the red rectangle (i.e., all sampling sites except Edischarge), and the sites characterized by significant differences in TE concentrations between sites are outlined with **

Fig 3 Daily fluxes of dissolved trace elements at Egly, Yvette and Viry sites for each sampling campaign in g d^{-1}

Fig 4 Daily fluxes of particulate trace elements estimated for each campaign at the Egly, Yvette and Viry (outlet) sites in g d^{-1} together with outlet water flow in m^3 s^{-1} during the sampling campaigns added in the figure of Pb fluxes

Fig 5 Contributions of Egly, Yvette and $Viry_{sub}$ subcatchments to the total dissolved TE exported during the June 2016 flood in % together with the water flow distribution

Figure1

Click here to access/download;Figure;Fig_1.jpg

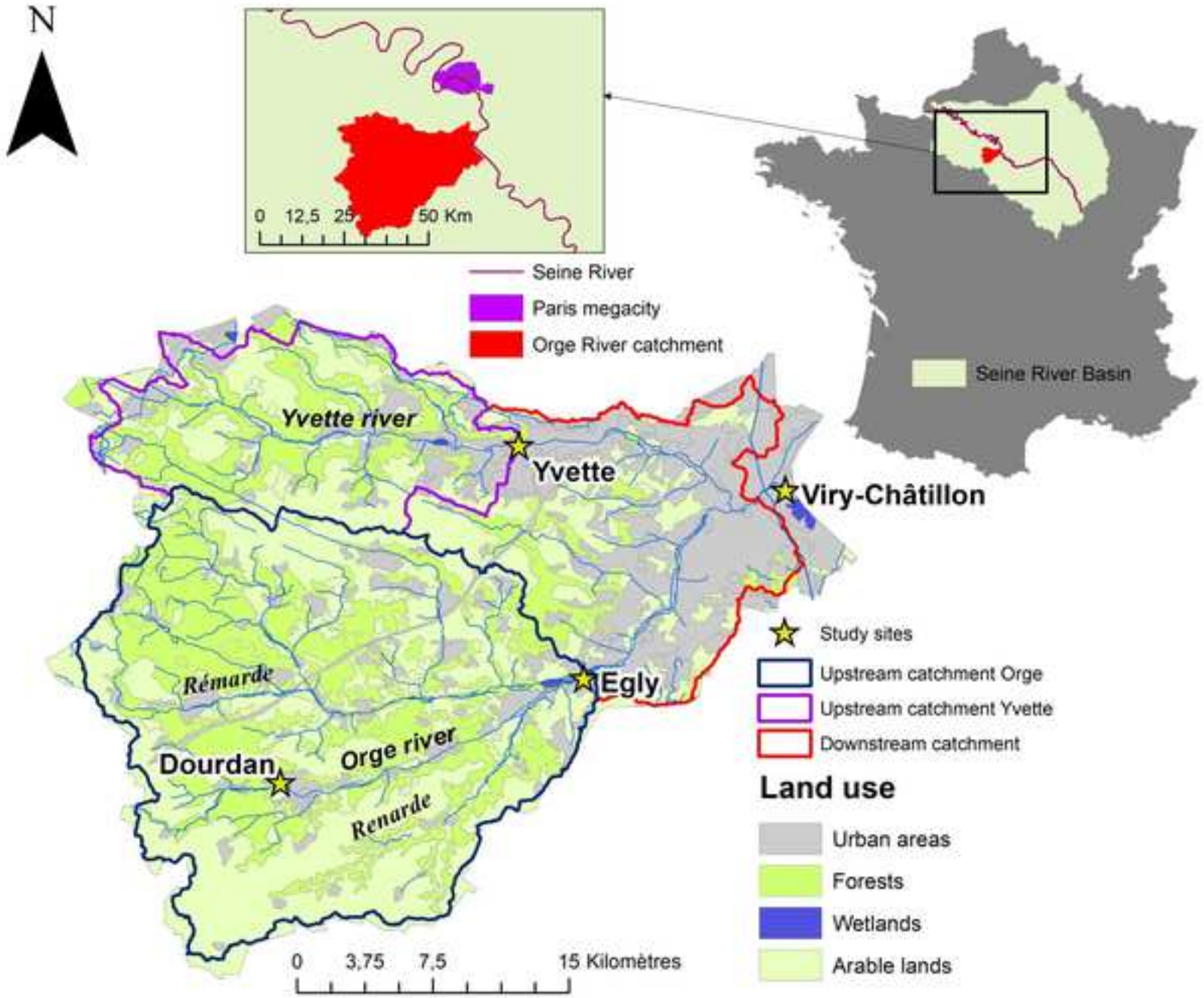

Figure2

Click here to access/download;Figure;Fig_2.jpg

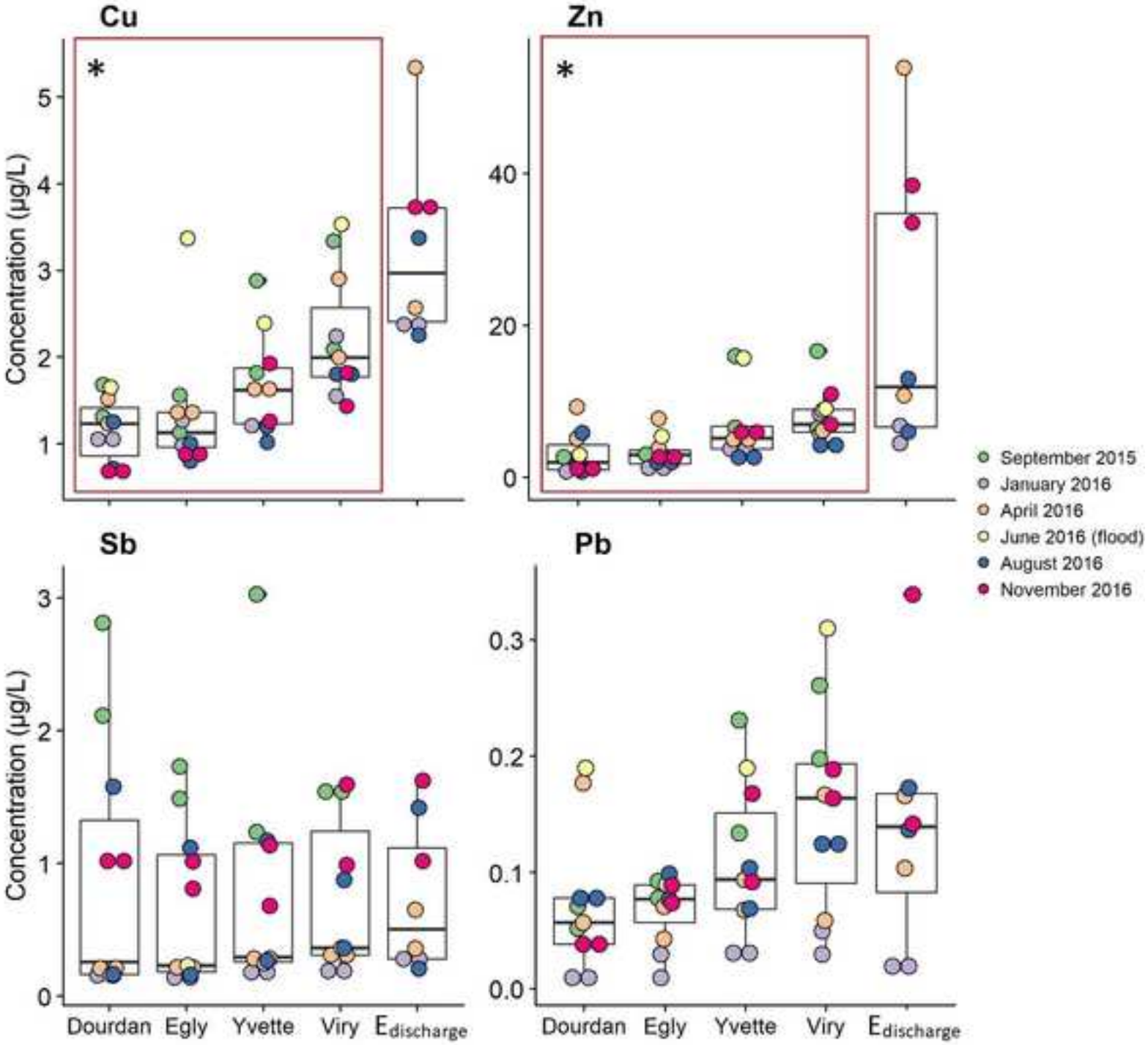

Figure3

Click here to access/download;Figure;Fig_3.jpg

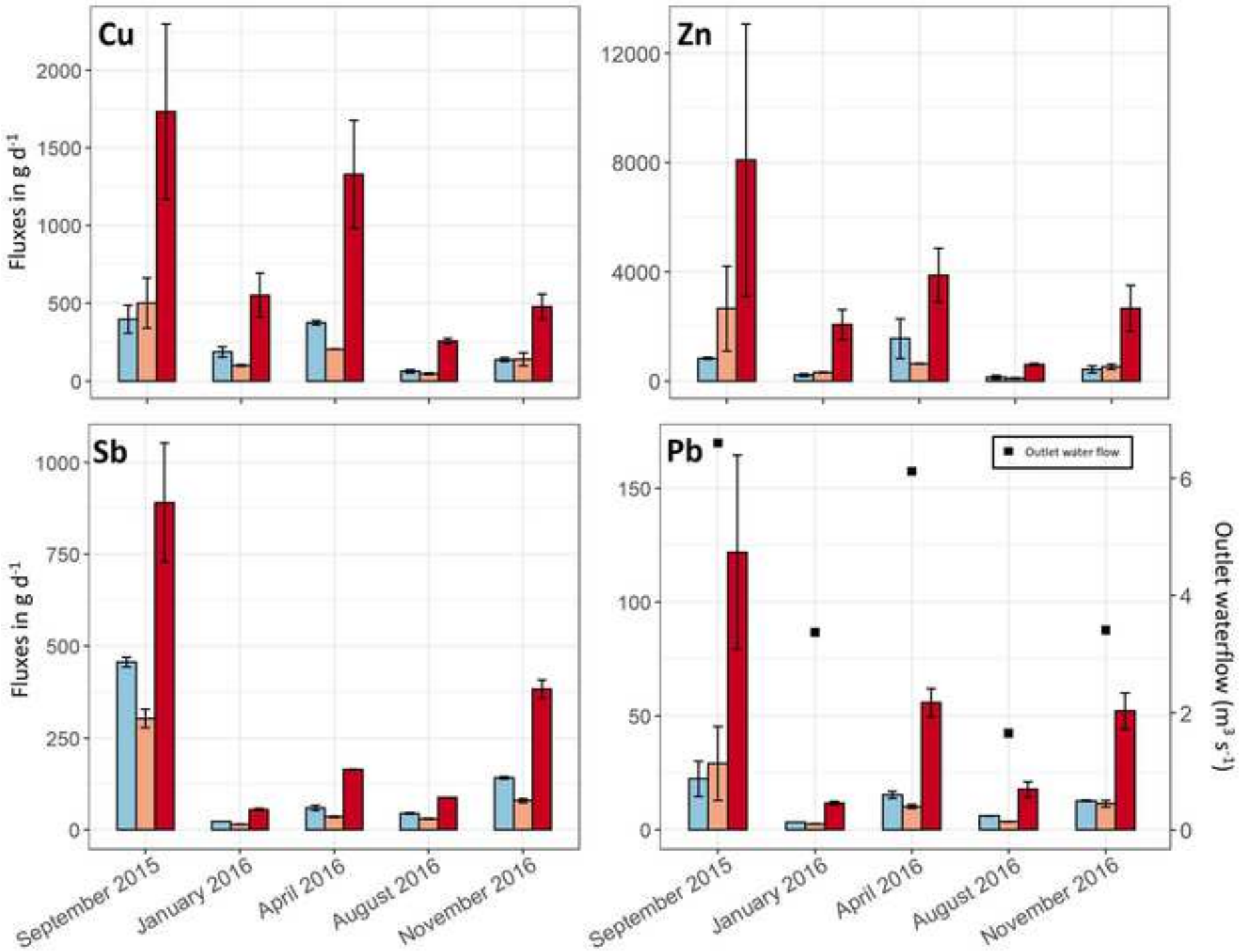

Figure4

Click here to access/download;Figure;Fig_4.jpg

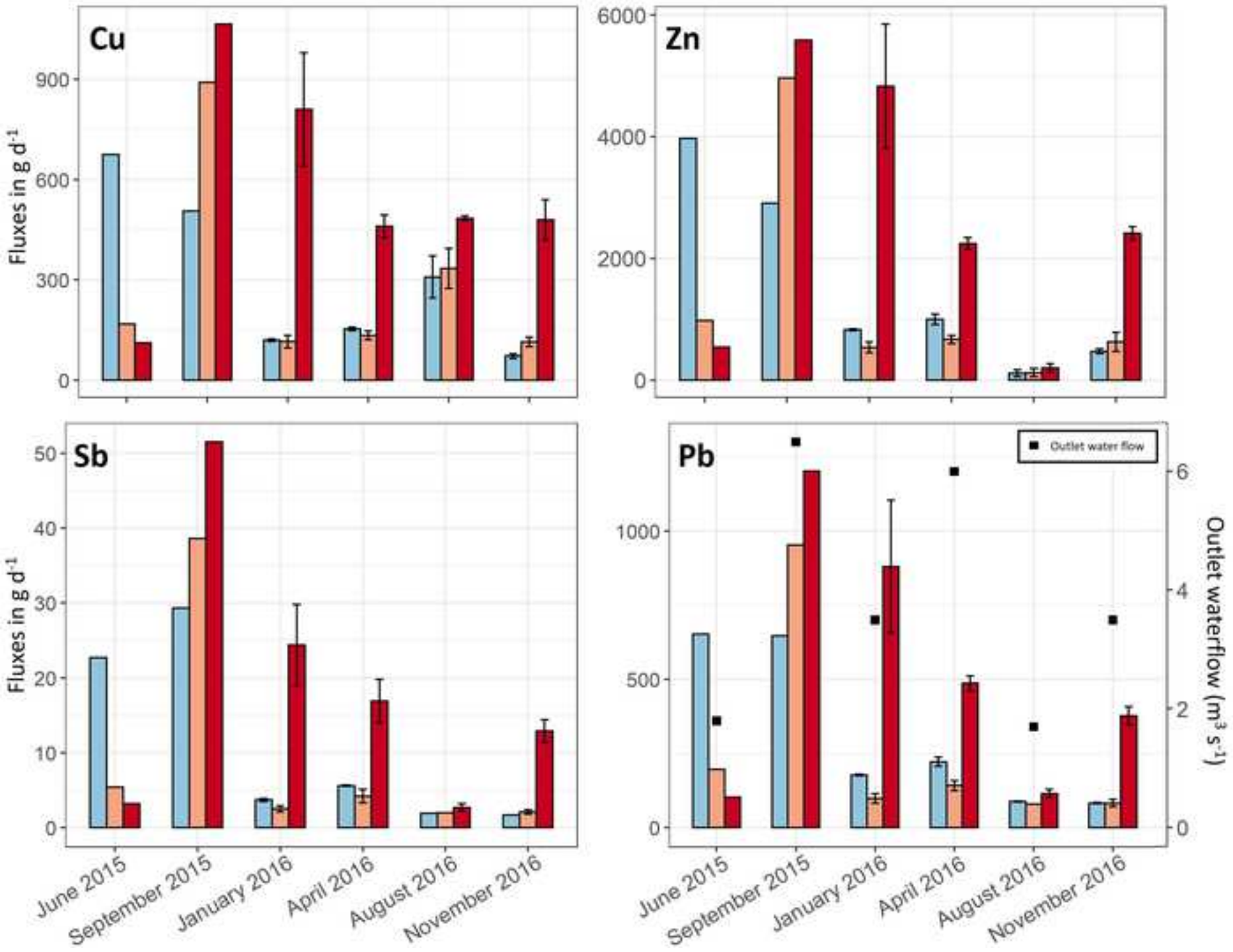

Figure5

Click here to access/download;Figure;Fig_5.jpg

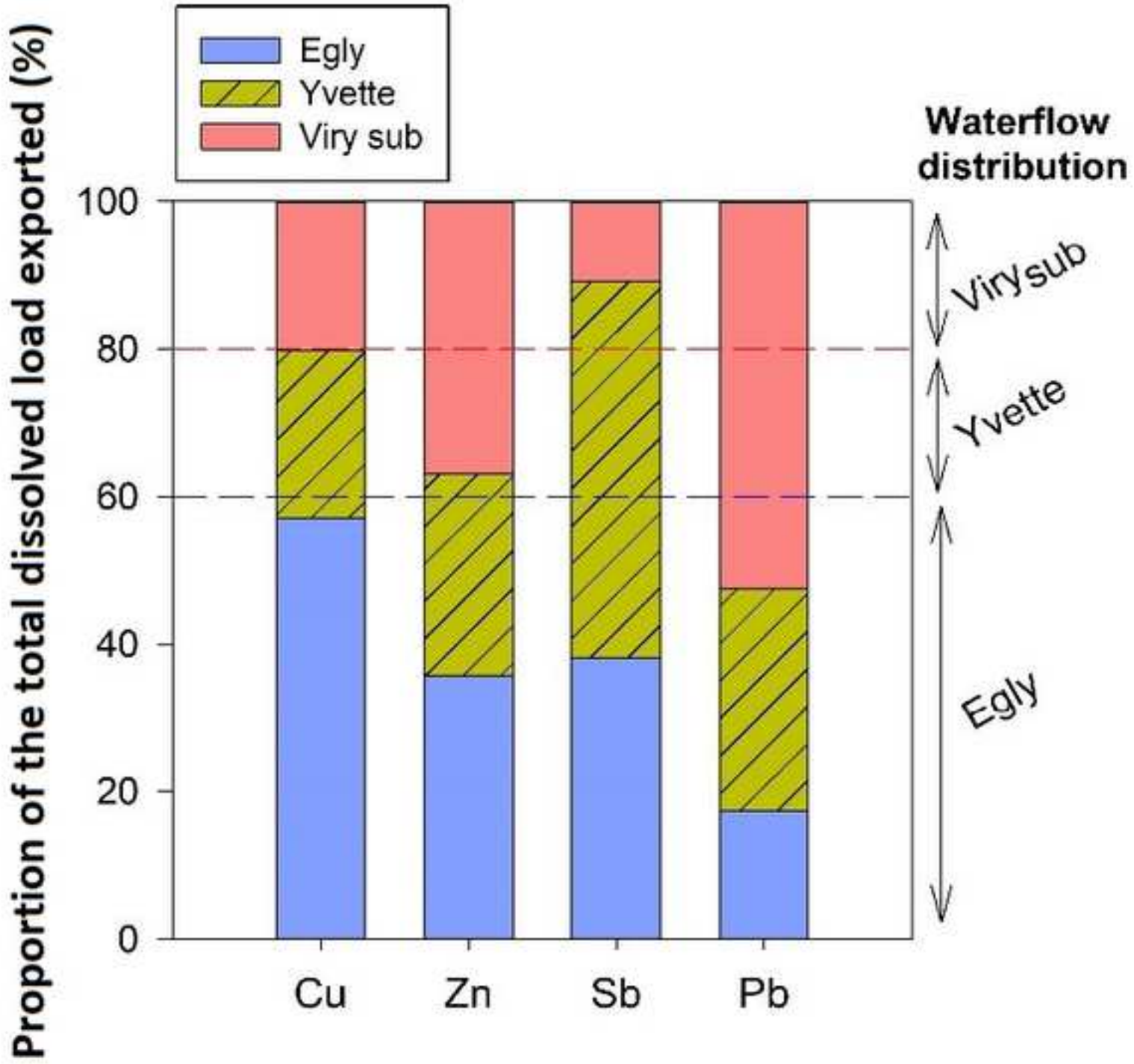

Supplementary material

Quantification of spatial and temporal variations in trace element fluxes originating from urban areas at a catchment scale

Claire Froger[*,1], Cécile Quantin[3], Louise Bordier[2], Gaël Monvoisin[3], Olivier Evrard[2], Sophie Ayrault[2]

*Corresponding author: claire.froger@inra.fr

Tel: ± 332 38 41 80 49

Address: INRA, 2163 avenue de la Pomme de Pin, 45075 ORLEANS CEDEX 2

[1] INRA, US1106 Unité Infosol, Centre de Recherches d'Orléans, CS 40001, Ardon, 45075 Orléans Cedex 2, France

[2] Laboratoire des Sciences du Climat et de l'Environnement (LSCE/IPSL), CEA-CNRS-UVSQ, Université Paris-Saclay, 91198 Gif-sur-Yvette, France

[3] Géosciences Paris Sud (GEOPS), Université Paris-Sud – CNRS-Université Paris-Saclay, 91400 Orsay, France

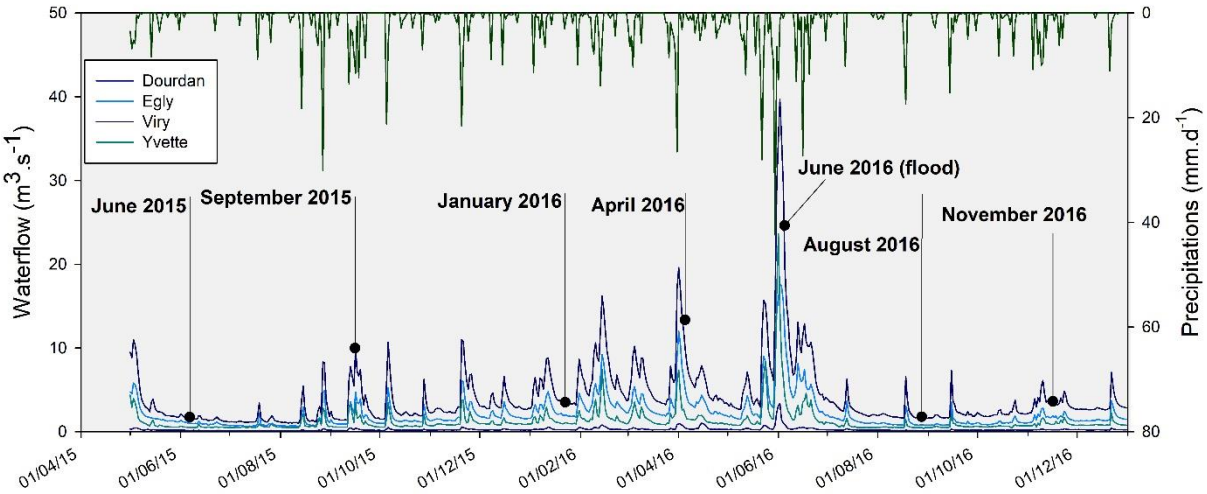

Figure S1: River flow and precipitation recorded in the Orge River catchment from January to December 2016 along with the sampling campaigns. Low flow periods: June 2015 (05/29/2015-06/05/2015) and August 2016 (08/24/2016-08/29/2016). Average discharge conditions: January 2016 (01/21/2016-01/25/2016) and November 2016 (11/16/2016-11/22/2016). High flow periods: September 2015 (09/16/2015-09/21/2015) and April 2016 (04/07/2016-04/11/2016). Extreme flooding: June 2016 (06/06/2016: water flow decrease).

Figure S 2 Sediment traps used in the study composed of PET plastic bottles drilled at their base to collect SPM by sedimentation. The plastic bottles were used for TE analysis in SPM.

Table S1: Major and trace element content in suspended particulate matter collected in the Orge River

Site	Campaign	g kg^{-1}												mg kg^{-1}							
		K	SD	Na	SD	Ca	SD	Mg	SD	Fe	SD	Al	SD	Cu	SD	Zn	SD	Sb	SD	Pb	SD
Dourdan	June 2015	13.6		5.5		25		3.8		37		50		32		141		1.3		42	
Dourdan	September 2015	10.9		4.2		20		2.9		20		40		20		85		1.0		29	
Dourdan	January 2016	11.0	0.4	3.2	1.2	23	6.1	4.1	1.0	46	16	56	12	81	77	353	203	1.4	0.1	54	9
Dourdan	April 2016	10.0	0.3	2.5	0.6	20	0.7	3.9	0.7	45	11	49	9	41	15	195	65	1.9	0.5	50	5
Dourdan	August 2016	11.4	0.5	3.4	0.6	18	4.6	4.3	0.9	41	8	59	9	142	98	81	67	1.3	0.0	54	4
Dourdan	November 2016	10.3	0.4	3.4	0.2	26	4.4	3.7	0.7	40	11	45	9	123	154	399	199	1.3	0.1	59	6
Dourdan	December 2016	10.6	0.3	3.9	0.1	21	0.6	3.1	0.2	28	1	43	1	25	0	137	1	1.0	0.0	46	0
Dourdan	June 2016 (flood)	12.8	0.01	2.3	0.0	17.4	1.3	5.8	0.01	59	0.3	79	0.7	69	1.2	381	4.8	1.5	0.01	81	0.3
Egly	June 215	14.9		5.2		35		5.8		40		54		76		448		2.6		74	
Egly	September 2015	11.1		4.0		39		3.4		22		35		44		252		2.5		56	
Egly	January 2016	11.6	0.4	3.3	0.8	38	2.1	4.5	1.0	32	10	48	8	52	11	348	105	1.6	0.3	75	16
Egly	April 2016	10.6	0.2	2.9	0.7	36	4.8	4.4	0.7	34	9	43	6	49	15	296	83	1.7	0.1	67	10
Egly	August 2016	11.6	0.1	3.7	0.5	34	6.6	4.5	0.6	29	5	48	5	218	152	124	114	1.6	0.1	72	7
Egly	November 2016	11.5	0.4	3.6	0.6	41	4.1	4.4	0.8	29	9	43	11	69	36	398	117	1.5	0.2	73	16
Egly	June 2016 (flood)	12.8		3.0		24		6.0		44		74		56		666		2.3		120	
Yvette	June 2015	13.4		4.8		49		4.1		26		40		43		252		1.4		51	
Yvette	September 2015	9.8		2.3		13		1.7		18		21		43		238		1.9		46	
Yvette	January 2016	11.2	0.8	3.2	0.4	26	3.3	4.9	1.7	46	21	55	16	88	39	409	88	1.9	0.2	75	17
Yvette	April 2016	10.2	0.1	2.5	0.7	21	1.2	4.5	0.9	41	13	49	13	73	18	360	78	2.1	0.2	75	16
Yvette	August 2016	11.6	0.1	3.6	0.5	24	6.6	4.7	0.6	34	5	47	5	302	152	176	114	2.1	0.1	82	7
Yvette	November 2016	10.9	1.1	3.9	0.5	29	4.9	4.2	0.2	34	8	40	4	109	50	645	302	2.1	0.1	81	15
Yvette	June 2016 (flood)	12.7	0.03	2.3	0.0	17	0.1	5.7	0.03	42	0.1	69	1	128	0.4	543	14	1.6	0.06	76	0.7
Viry	June 2015	11.9		4.2		47		5.9		30		42		84		408		2.4		78	
Viry	September 2015	9.6		2.6		21		2.3		11		21		39		203		1.9		44	

Viry	January 2016	11.5	0.1	2.4	0.6	39	2.2	7.1	0.3	41	6	55	5	107	5	640	92	3.2	0.6	120	28
Viry	April 2016	10.5	0.4	2.7	0.7	30	3.2	5.1	0.7	34	8	45	9	84	23	402	89	3.3	0.9	88	13
Viry	August 2016	9.8	0.6	2.6	0.5	47	8.2	4.5	0.3	23	4	32	4	403	300	205	155	2.5	0.4	102	13
Viry	November 2016	10.9	0.5	3.1	0.7	41	1.8	5.4	0.6	29	4	40	2	134	51	637	125	3.6	0.5	102	17
Viry	June 2016 (flood)	12.4		3.8		28		6.3		39		63		108		472		2.1		84	

Table S 2 SPM enrichment factors (EF) in Cu, Zn, Pb and Sb. Already published in Froger et al., (2018)

EF		**Cu**	**Zn**	**Sb**	**Pb**
Dourdan	June 2015	2.7	1.9	2.2	2.3
Dourdan	September 2015	2.1	1.4	2.1	2.0
Dourdan	January 2016	6.1	4.2	2.1	2.7
Dourdan	April 2016	3.6	2.7	3.2	2.8
Dourdan	August 2016	10.2	0.9	1.8	2.5
Dourdan	November 2016	11.6	6.0	2.4	3.6
Dourdan	December 2016	2.5	2.1	1.9	3.0
Dourdan	June 2016 (flood)	3.7	3.2	1.6	2.8
Egly	June 215	6.0	5.6	4.0	3.8
Egly	September 2015	5.3	4.8	5.9	4.4
Egly	January 2016	4.6	4.9	2.8	4.3

Egly	April 2016	4.8	4.6	3.3	4.3
Egly	August 2016	19.3	1.7	2.8	4.1
Egly	November 2016	6.8	6.2	2.9	4.7
Egly	June 2016 (flood)	3.2	6.1	2.6	4.5
Yvette	June 2015	4.6	4.2	2.9	3.5
Yvette	September 2015	8.7	7.6	7.5	6.0
Yvette	January 2016	6.8	5.0	2.9	3.8
Yvette	April 2016	6.3	4.9	3.6	4.2
Yvette	August 2016	27.3	2.5	3.7	4.8
Yvette	November 2016	11.6	10.8	4.3	5.6
Yvette	June 2016 (flood)	7.9	5.3	1.9	3.0
Viry	June 2015	8.5	6.5	4.7	5.1
Viry	September 2015	7.9	6.5	7.5	5.8
Viry	January 2016	8.3	7.8	4.8	6.0
Viry	April 2016	7.9	6.0	6.1	5.4
Viry	August 2016	53.5	4.3	6.5	8.8
Viry	November 2016	14.2	10.7	7.5	7.0
Viry	June 2016 (flood)	7.3	5.0	2.8	3.7

Table S3: Major ion and trace element concentrations in the dissolved compartment of the Orge River

Site	Campaign	mg L^{-1}																µg L^{-1}							
		K	SD	Na	SD	Ca	SD	Mg	SD	F	SD	Cl^-	SD	NO_3^-	SD	SO_4^{2-}	SD	Cu	SD	Zn	SD	Sb	SD	Pb	SD
Dourdan	September 2015	2.4	0.0	26.0	1.7	82	11.6	6.1	0.7	0.14	0.01	47	0.9	11.4	2.0	38	0.2	1.5	0.3	2.7	1.0	2.5	0.5	0.06	0.01
	January 2016	2.2	0.1	16.3	0.1	96	0.0	7.0	0.0	0.10	0.00	33	0.4	22.0	0.3	33	0.7	1.1	0.1	0.8	0.3	0.2	0.0	0.01	0.00
	April 2016	2.1	0.1	18.6	1.8	83	3.4	6.0	0.2	0.08		34	3.0	19.7	2.6	29	0.2	1.4	0.2	7.2	3.0	0.2	0.1	0.12	0.08
	August 2016	2.2	0.0	14.5	0.0	80	1.6	7.3	0.0	0.04	0.00	27	0.1	14.5	0.8	29	0.0	1.0	0.4	3.4	3.6	0.9	1.0	0.08	0.00
	November 2016	3.1	0.1	19.7	1.0	99	1.2	7.5	0.1	0.01	0.00	36	1.8	15.0	1.0	33	0.3	0.7	0.0	1.1	0.2	1.0	0.1	0.04	0.00
	June 2016 (flood)	3.4		14.2		70		5.7		0.10		23		14.2		25		1.7		3.0		0.16		0.19	
Egly	September 2015	3.1	0.1	17.2	2.7	85	12.4	7.3	0.9	0.16	0.00	33	5.2	14.8	2.2	37	5.3	1.3	0.3	3.1	0.1	1.6	0.2	0.09	0.01
	January 2016	3.0	0.4	15.8	0.8	106	7.4	9.0	0.7	0.15	0.00	34	0.0	24.3	0.2	43	0.0	1.1	0.2	1.3	0.3	0.1	0.0	0.02	0.01
	April 2016	3.7	0.1	19.5	0.6	101	2.6	8.8	0.0	0.12	0.04	35	0.9	21.5	0.1	44	0.0	1.4	0.0	5.8	2.7	0.2	0.0	0.06	0.02
	August 2016	3.2	0.1	15.6	0.1	89	0.2	8.7	0.1	0.04	0.01	30	0.3	22.5	0.5	33	0.4	0.9	0.1	2.0	1.0	0.6	0.7	0.09	0.02
	November 2016	4.5	1.0	17.0	0.2	99	6.2	8.9	0.0	0.02	0.01	32	0.7	21.0	1.7	39	0.6	0.9	0.1	2.7	0.8	0.9	0.1	0.08	0.01
	June 2016 (flood)	4.4		16.3		90		8.3		0.21		28		15.4		46		3.4		5.4		0.23		0.09	
Yvette	September 2015	3.7	1.0	17.5	7.1	67	24.4	6.8	2.9	0.16	0.05	28	12.4	9.0	4.0	54	20.1	2.4	0.7	11.3	6.6	2.1	1.3	0.18	0.07
	January 2016	4.2	0.1	20.4	2.1	76	4.3	7.7	0.5	0.11	0.00	31	1.6	11.8	0.7	53	0.9	1.6	0.1	5.0	0.2	0.3	0.0	0.08	0.00
	April 2016	4.2	1.0	20.4	1.2	76	0.9	7.7	0.3	0.11	0.01	31	2.1	11.8	0.7	53	1.1	1.6	0.0	5.0	0.2	0.3	0.0	0.08	0.02
	August 2016	4.6	0.1	29.6	0.9	87	0.3	11.0	0.3	0.07	0.00	44	1.2	11.3	0.4	63	1.4	1.1	0.1	2.6	0.4	0.7	0.6	0.09	0.02
	November 2016	6.2	0.7	27.1	0.4	91	4.9	10.0	0.5	0.03		41	1.6	12.5	0.9	64	3.0	1.6	0.5	6.0	1.1	0.9	0.3	0.13	0.05
	June 2016 (flood)	4.1		14.9		74		6.0		0.14		15		11.5		45		3.9		12.2		0.9		0.46	
Viry	September 2015	4.4	0.9	19.5	4.6	71	20.3	7.3	2.4	0.18	0.04	33	8.5	10.6	3.1	57	16.9	2.7	0.9	11.6	7.1	1.5	0.1	0.23	0.04
	January 2016	4.6	0.1	25.9	1.9	120	8.3	11.5	0.1	0.20	0.00	44	3.5	25.2	3.0	81	10.0	1.9	0.5	7.1	1.9	0.2	0.0	0.04	0.01
	April 2016	5.0	0.6	23.8	1.5	98	3.9	10.2	0.6	0.13	0.01	39	2.9	17.5	0.7	74	2.2	2.4	0.6	7.5	1.9	0.3	0.0	0.11	0.08
	August 2016	5.5	0.4	29.9	4.8	107	13.2	11.6	0.1	0.10	0.02	50	8.2	20.9	4.6	80	10.5	1.8	0.1	4.3	0.2	0.6	0.4	0.12	0.00
	November 2016	8.0	1.6			102	1.8	11.7	1.4	0.03	0.03	45	0.2	16.0	0.5	70	4.9	1.6	0.3	9.0	2.8	1.3	0.4	0.18	0.02
	June 2016 (flood)	5.4		17.4		88		9.4		0.23		28		14.8		70		3.5		9.1		0.36		0.31	

Table S4: Dissolved/total partition of trace elements in the water column of the Orge River for every campaign and at each site based on instantaneous water samples

Site	Campaign	Proportion of TE in the dissolved compartment (in %)							
		Cu	SD	Zn	SD	Sb	SD	Pb	SD
Dourdan	September 2015	62	4	37	9	98	0	4	1
Dourdan	January 2016	30	23	5	3	76	5	1	0
Dourdan	April 2016	73	2	74	5	90	1	17	10
Dourdan	June 2016 (flood)	49	0	24	0	81	0	9	0
Dourdan	August 2016	11	3	55	32	84	18	3	1
Dourdan	November 2016	60	12	38	20	99	0	15	9
Egly	September 2015	42	6	23	1	96	0	4	0
Egly	January 2016	55	15	17	10	83	6	1	0
Egly	April 2016	68	6	58	9	91	1	6	2
Egly	June 2016 (flood)	73	0	26	0	81	0	3	0
Egly	August 2016	11	1	57	11	88	12	5	1
Egly	November 2016	66	1	51	14	99	0	16	4
Yvette	September 2015	36	7	32	13	89	6	4	1
Yvette	January 2016	43	14	41	8	93	2	3	1
Yvette	April 2016	60	1	50	2	91	0	7	1
Yvette	June 2016 (flood)	51	15	46	7	87	2	11	3
Yvette	August 2016	9	2	58	5	89	9	4	1
Yvette	November 2016	64	17	55	17	98	2	20	11
Viry	September 2015	56	8	49	16	95	0	10	2
Viry	January 2016	57	36	47	39	79	21	5	6
Viry	April 2016	82	19	59	13	89	0	10	9
Viry	June 2016 (flood)	54	8	83	7	80	12	13	1
Viry	August 2016	26	18	77	16	96	0	11	5
Viry	November 2016	47	21	51	30	95	5	14	12

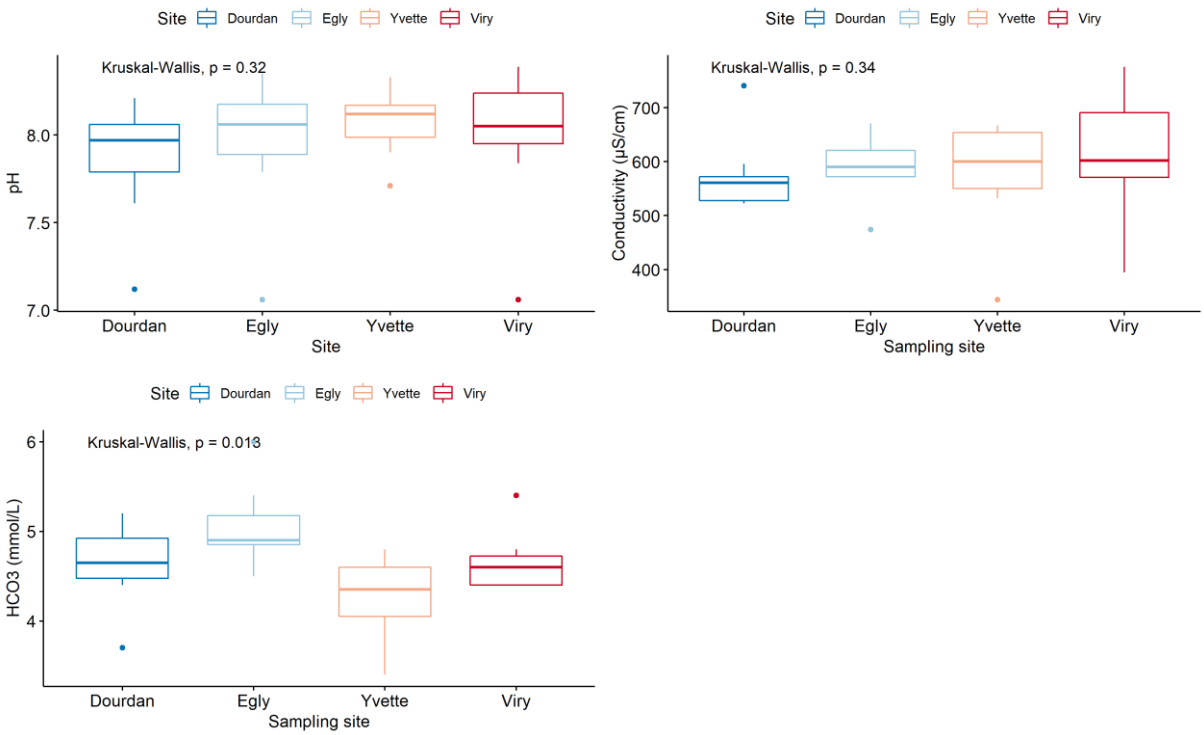

Figure S 3 Boxplots of pH, conductivity and HCO_3^- by sampling site, from up to donwtream along with the results of Kruskal-Wallis tests

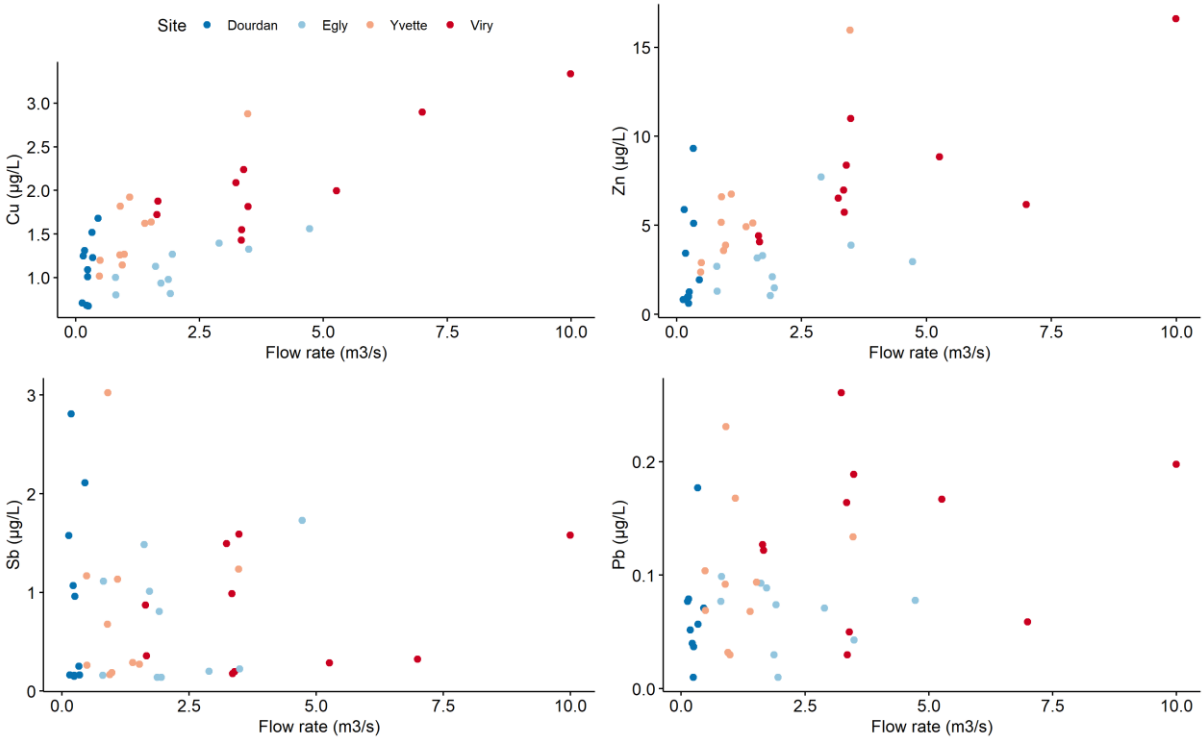

Figure S 4 Trace element concentrations in the dissolved compartment by flow rate displayed by sampling site.

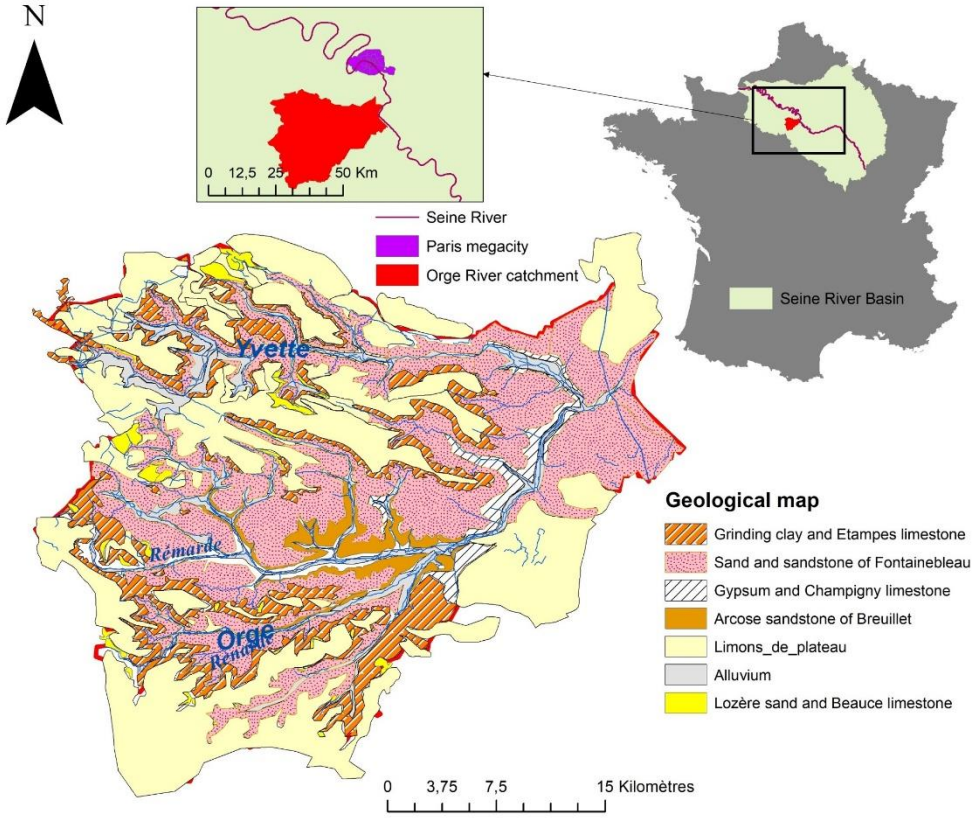

Figure S 5 Map of the Orge catchment geology

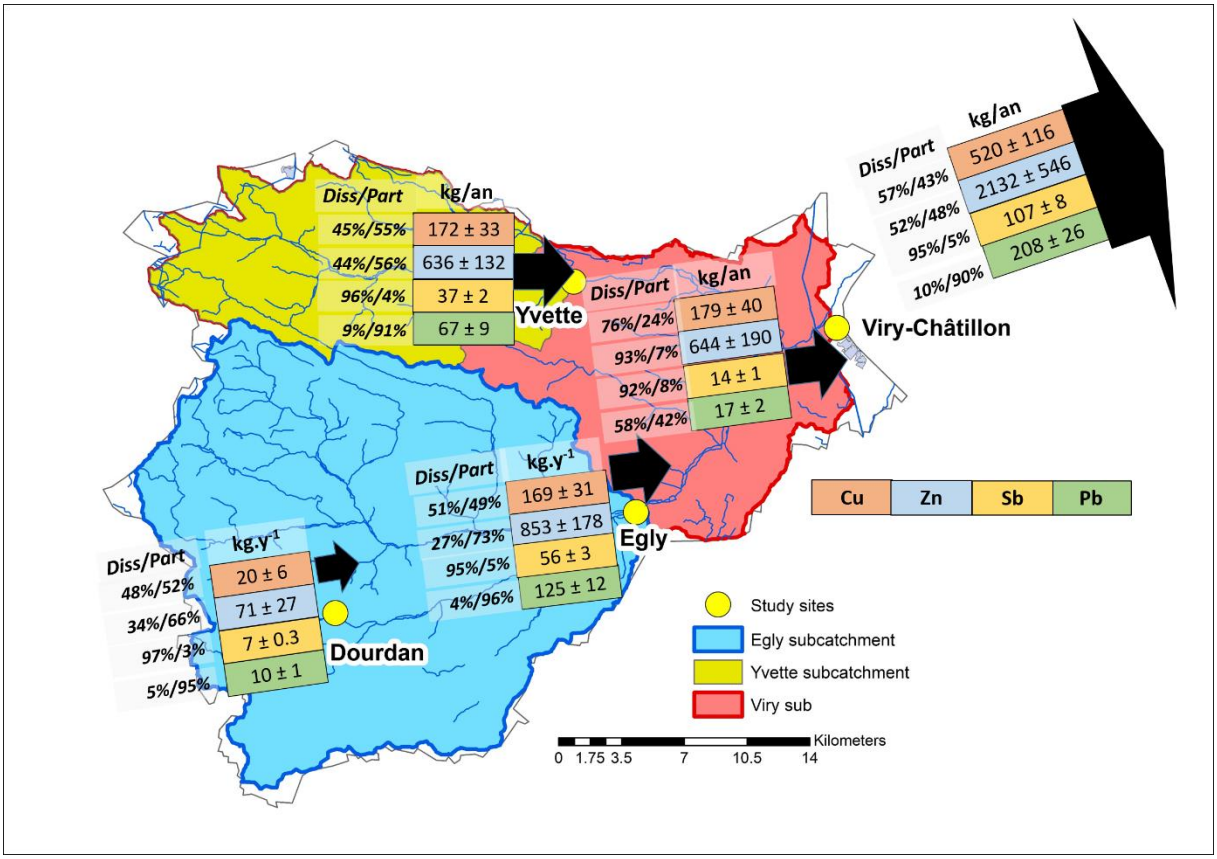

Figure S6: Detailed annual fluxes of Cu, Zn, Sb and Pb for each subcatchment of the Orge River

Table S5: Detailed daily particulate fluxes of Cu, Zn Sb and Pb estimated at each sampling site for every campaign

		SPM (mg L^{-1})	Water flow (m^3 s^{-1})	Fluxes in g d^{-1}				SD in g d^{-1}			
				Cu	Zn	Sb	Pb	Cu	Zn	Sb	Pb
Egly	June 2015	84	0.2	675	3972	23	652	-[a]	-	-	-
	September 2015	42	3.2	506	2908	29	646	-	-	-	-
	January 2016	13	1.9	122	816	4	176	27	247	0.66	38
	April 2016	12	3.2	157	938	5	212	47	262	0.40	32
	August 2016	17	0.8	263	149	2	87	184	138	0.10	8
	November 2016	7	1.8	77	443	2	82	40	131	0.25	17
Yvette	June 2015	76	0.6	167	974	5	197	-	-	-	-
	September 2015	144	1.7	891	4963	39	953	-	-	-	-
	January 2016	13	1.0	129	599	3	109	57	129	0.36	25
	April 2016	14	1.4	125	618	4	129	31	135	0.29	27
	August 2016	23	0.5	291	170	2	79	147	110	0.08	6
	November 2016	11	1.0	124	738	2	93	57	346	0.15	18

Viry	June 2015	9	1.8	111	539	3	103	-	-	-	-
	September 2015	49	6.5	1065	5583	51	1202	-	-	-	-
	January 2016	22	3.5	930	5550	28	1037	43	799	4.82	244
	April 2016	10	6.0	484	2311	19	505	131	512	5.33	73
	August 2016	7	1.7	489	248	3	124	364	189	0.47	16
	November 2016	11	3.5	522	2490	14	398	198	488	1.86	67

[a]: (-) indicates that no uncertainties could be calculated for the fluxes

Table S6: Daily fluxes of dissolved trace elements in g.d^{-1} estimated for each campaign

		Water flow (m^3 s^{-1})	**Fluxes in g d^{-1}**				**SD in g d^{-1}**			
			Cu	Zn	Sb	Pb	Cu	Zn	Sb	Pb
Egly	September 2015	3.2	397	824	456	22	90	40	13	8
	January 2016	1.9	186	213	23	3	34	50	0	0
	April 2016	3.2	374	1550	60	15	14	725	7	1
	August 2016	0.8	63	139	45	6	10	69	2	0
	November 2016	1.8	137	420	142	13	13	130	4	0
Yvette	September 2015	1.7	502	2652	303	29	160	1556	25	16
	January 2016	1.0	100	310	15	3	5	13	1	0
	April 2016	1.4	205	633	36	10	1	19	1	1
	August 2016	0.5	47	111	30	4	5	16	1	0
	November 2016	1.0	139	517	80	11	41	98	5	1
Viry	September 2015	6.5	1733	8084	891	122	564	4983	162	43
	January 2016	3.5	552	2061	55	12	142	544	3	1
	April 2016	6.0	1329	3875	164	56	347	980	1	6
	August 2016	1.7	257	607	88	18	16	34	1	3
	November 2016	3.5	480	2661	382	52	81	841	26	8

Table S7: Concentrations of dissolved and particulate Cu, Zn, Sb and Pb measured on June 6, 2016

	Water flow ($m^3 s^{-1}$)	**SPM (mg L^{-1})**	**Dissolved concentrations in µg L^{-1}**				**Particulate concentrations in mg kg^{-1}**			
			Cu	Zn	Sb	Pb	Cu	Zn	Sb	Pb
Dourdan	0.6	76	1.7	3.0	0.2	0.2	69	381	1.5	81
Egly	9.1	96	3.4	5.4	0.2	0.1	56	666	2.3	120
Yvette	3.1	80	3.9	12.2	0.9	0.5	128	543	1.6	76
Viry	15.2	81	3.5	9.1	0.4	0.3	108	472	2.1	84